Ontogenetic changes in limb posture, kinematics, forces, and joint moments in American alligators (*Alligator mississippiensis*)

Masaya Iijima[1,2,*], V. David Munteanu[1], Ruth M. Elsey[3] and Richard W. Blob[1,*]

[1]Department of Biological Sciences, Clemson University, SC 29634, USA. [2]Nagoya University Museum, Furocho, Chikusa-Ku, Nagoya, Aichi 464-8601, Japan. [3]Louisiana Department of Wildlife and Fisheries, Rockefeller Wildlife Refuge, 5476 Grand Chenier Highway, Grand Chenier, LA 70643, USA.

*Authors for correspondence (miijima8@gmail.com; rblob@clemson.edu)

Key words: locomotion, biomechanics, ground reaction force, center of mass, archosaur

Summary: Larger alligators walk with more upright limb posture and smaller size-normalized joint moments. Limb forces are more hindlimb dominant in larger alligators, possibly due to a more posterior center of mass and less compliant hindlimbs.

ABSTRACT

As animals increase in size, common patterns of morphological and physiological scaling may require them to perform behaviors such as locomotion while experiencing a reduced capacity to generate muscle force and an increased risk of tissue failure. Large mammals are known to manage increased mechanical demands by using more upright limb posture. However, the presence of such size-dependent changes in limb posture has rarely been tested in animals that

use non-parasagittal limb kinematics. Here, we used juvenile to subadult American alligators (total length 0.46–1.27 m, body mass 0.3–5.6 kg) and examined their limb kinematics, forces, joint moments, and center of mass to test for ontogenetic shifts in posture and limb mechanics. Larger alligators typically walked with a more adducted humerus and femur and a more extended knee. Normalized peak joint moments reflected these postural patterns, with shoulder and hip moments imposed by the ground reaction force showing relatively greater magnitudes in the smallest individuals. Thus, as larger alligators use more upright posture, they incur relatively smaller joint moments than smaller alligators, which could reduce the forces that the shoulder and hip adductors of larger alligators must generate. The center of mass (CoM) shifted nonlinearly from juveniles through subadults. The more anteriorly positioned CoM in small alligators, together with their compliant hindlimbs, contributes to their higher forelimb and lower hindlimb normalized peak vertical forces in comparison to larger alligators. Future studies of alligators that approach maximal adult sizes could give further insight into how animals with non-parasagittal limb posture modulate locomotor patterns as they increase in mass and experience changes in the CoM.

INTRODUCTION

Body size is one of the most important traits that influences the terrestrial locomotor capacities of tetrapods. Although larger animals can take advantage of the reduced weight-specific cost of locomotion (Heglund and Taylor, 1988; Kram and Taylor, 1990; Reilly et al., 2007), they must also accommodate mechanical limitations of the musculoskeletal system. If the shapes and properties of anatomical structures were geometrically similar among animals of different sizes, then larger ones would have to cope with reduced force generating capacity of their muscles, and

an increased risk of tissue failure (Biewener and Patek, 2018). This is because the demands placed on muscle and bone typically increase in proportion to body mass, or L^3, but muscle force generation and the peak stresses that muscle, tendon, and bone can accommodate would scale in proportion to their cross-sectional areas, or L^2 (Biewener and Patek, 2018; McMahon, 1973, 1975a). Animals use multiple strategies to deal with such size-dependent increases in mechanical demands, with the strategies that a species uses appearing to relate to whether it employs parasagittal or non-parasagittal limb kinematics (Biewener, 1983; Cieri et al., 2021).

Mammals that use parasagittal locomotion show a tendency to change limb posture with increasing body mass: smaller species of mammals use more crouched limb posture, whereas larger species use more erect posture (Biewener, 1983; Gray, 1968; Gregory, 1912). Because the vector of the ground reaction force (GRF) aligns more closely with erect limb bones, the effective mechanical advantage (EMA) of limb muscles (i.e., the ratio of the muscle moment arm to the GRF moment arm) is greater in large, upright mammals (Biewener, 1983, 1989, 1990, 2005, 2015). Together with generally positive scaling of muscle and bone cross-sectional areas versus body mass (Alexander et al., 1979a, 1981; Bertram and Biewener, 1990; Campione and Evans, 2012; McMahon, 1975b; Pollock and Shadwick, 1994), positive EMA scaling ($\propto mass^{0.25}$: Biewener, 1989, 2005) contributes to maintaining similar magnitudes of bone and muscle stresses across wide size ranges of mammals (Biewener, 1990, 2005). Birds show similar size-dependent trends for limb posture (more upright hindlimbs in larger species), which also result in the increased EMA of hindlimb muscles (Daley and Birn-Jeffery, 2018; Gatesy and Biewener, 1991).

Among tetrapods that use non-parasagittal limb posture, varanid and iguanid lizards show positive scaling of limb muscle and bone cross-sectional areas (Blob, 2000; Christian and Garland, 1996; Cieri et al., 2020; Dick and Clemente, 2017), but limb posture during running seems to be similar across species that span a wide range of body masses (Clemente et al., 2011). Although duty factor increases and locomotor speed decreases among larger varanids (Cieri et al., 2021; Clemente et al., 2012), it remains uncertain whether their muscle and bone stresses are maintained at similar magnitudes. Bone stress estimations based on ground reaction forces and muscle forces in green iguanas suggested that femoral bending stresses would be higher when using more upright limb posture (Blob and Biewener, 2001), which might explain why larger lizards do not use more upright stance.

Crocodylians are large quadrupeds that use diverse limb postures from a belly walk to a high walk, although the belly walk is primarily used for a transition to and from high walk posture (Brinkman, 1980; Gatesy, 1991; Reilly and Elias, 1998). Ancestrally, early pseudosuchians (crocodylian-line archosaurs that first appeared in the Early Triassic: Nesbitt, 2011) showed morphological adaptations suited for parasagittal limb posture, including downward facing acetabula (Benton and Clark, 1988; Bonaparte, 1984; Parrish, 1986, 1987). Because of a likely secondary acquisition of non-parasagittal limb posture among modern crocodylians, limb kinematics (e.g. femur and knee angles and movements during stance) of the high walk are intermediate between kinematics of parasagittal and sprawling posture in the postural continuum (Charig, 1972; Gatesy, 1991; Nyakatura et al., 2019; Reilly and Elias, 1998). Therefore, studies of size-dependent changes in limb geometries and locomotion in crocodylians can provide a distinct insight into the strategies used to address increasing mechanical demands with larger body size among animals that use postures intermediate between strictly sprawling and parasagittal.

Previous intra- and interspecific comparisons of limb muscles and bones in crocodylians showed an overall geometric similarity of limb muscle cross-sectional areas and positive allometry of limb bone diameters and circumferences versus lengths, the latter of which might help maintain similar bone stresses across a range of body sizes (Allen et al., 2010; Blob, 2000; Iijima and Kubo, 2019). Meanwhile, bending stresses of the femur increase with more upright posture in juvenile alligators, which might be explained by greater activation of knee extensor muscles that compress the dorsal cortex of the femur during upright stance (Blob and Biewener, 1999; Reilly and Blob, 2003). However, it remains unknown whether small and large alligators use similar limb postures, as found for interspecific comparisons of monitor lizards (Clemente et al., 2011).

In this study, we measured fore- and hindlimb kinematics and kinetics across American alligators ranging from small juveniles to subadults (body mass 0.3–5.6 kg). By integrating measurements of limb kinematics with speed and stride parameters, ground reaction forces, joint moments, and center of mass, we tested for ontogenetic shifts in posture and limb mechanics in alligators to evaluate the generality of patterns among non-parasagittal tetrapods. If alligators use a similar posture throughout ontogeny, it could lend support to the hypothesis that differences in limb anatomy between mammals and non-avian sauropsids (e.g., alligators and iguanas) lead to differences in how hindlimb muscles and bone loading are modulated over the limb posture gradient: the use of more upright posture does not help non-avian sauropsids to reduce bone stresses (Reilly and Blob, 2003). Conversely, if larger alligators use more upright posture as shown in the interspecific comparisons of mammals, the reason as to why they choose a posture that could increase bone stresses would require explanation.

MATERIALS AND METHODS

Animals

Twelve juvenile to subadult American alligators, *Alligator mississippiensis* (Daudin, 1802), were provided by the Rockefeller Wildlife Refuge, Grand Chenier, LA, USA. These animals were hatched in the wild and collected by Louisiana Department of Wildlife and Fisheries alligator program staff biologists and technicians. Animals used for walking trials were divided into three size classes: small (n = 3, total length 0.46–0.48 m, body mass 0.23–0.26 kg), medium (n = 3, total length 0.81–0.90 m, body mass 1.40–2.06 kg), and large (n = 1, total length 1.27 m, body mass 5.64 kg). Sexes and ages of animals were unknown. The sampled range of body mass is narrower than that in the previous interspecific comparison of crocodylian locomotion (Hutchinson et al., 2019). However, the large individuals approach the maximum size that we could keep in our animal facility. Animals were individually housed at Clemson University in enclosures filled with shallow water in a greenhouse vivarium facility, with ambient lighting and humidity, daytime temperatures between 23–38 °C, and periodically open roof panels to provide natural sunlight and UV. Small and medium individuals were fed commercial pellets for crocodylians (Mazuri crocodilian diet-small), and large individuals were offered pellets, live feeder fish, or pieces of boneless chicken or pork twice a week. Animal care and experimental procedures were approved by Clemson University IACUC (protocol 2019-037). Measurements of just center of mass were obtained from 33 additional individuals (total length 0.47–1.55 m, body mass 0.25–8.00 kg) housed at Clemson University and the Rockefeller Wildlife Refuge.

Data collection and processing

Walking trials were conducted in a wooden trackway fitted with a force plate that was made level with the walking surface, and with a clear panel on one side to facilitate video imaging. Room temperature was controlled at 23 °C, and animals were allowed to rest under heat lamps for several minutes between the trials. Animals were filmed simultaneously from lateral and dorsolateral views with two digitally synchronized Phantom v.5.1 high-speed cameras (Vision Research, Wayne, NJ, USA) at 100 Hz. Single-foot ground reaction forces (GRFs) of fore- and hindlimbs were recorded at 5000 Hz from either a custom-built K&N Scientific (Guilford, VT, USA) force plate (see Butcher and Blob, 2008 for specifications) or a Kistler (Novi, MI, USA) force plate (type 9260AA3Y0500), using custom LabVIEW routines (v.6.1, National Instruments, Austin, TX, USA). Plate calibrations were conducted manually (K&N Scientific plate) or from verified manufacturer specifications (Kistler plate) each day of trials. Force data were synchronized with video using a trigger that simultaneously sent a 1.5 V square-wave pulse to a force trace channel and a light pulse to video. Raw force signals were processed by averaging values to produce samples at 50 Hz. Force baselines were corrected to zero using data 0.02 s before foot touchdown, as indicated by video frames. Force data and kinematics were analyzed only for the stance phase duration of a footfall.

To obtain 3D coordinates of the anatomical landmarks for kinematic measurements, white dots of correction fluid were painted on the right forelimb (metacarpophalangeal joint of digit III, wrist, elbow, and shoulder joints), right hindlimb (metatarsophalangeal joint of digit III, ankle, knee, and hip joints), and the midline of the trunk (medial to the right shoulder and hip, and three equidistant points between them). The 3D space through which animals walked was calibrated via DLTcal5 software using toy building bricks of known dimensions, with 3D coordinates of landmarks digitized using DLTdv7 (Hedrick, 2008) in MATLAB R2019b. Frames during stance

(touchdown to toe-off) of each limb were digitized at various rates depending on the stance duration. Walking speed during a single stride was measured by tracking the landmarks on the midline of the body. Speed during an entire stride, rather than just stance phase, was measured to evaluate steady speed over a longer duration. Only steady speed and straight walks with the placement of a whole foot on the force plate were chosen for analyses. Steady speed was evaluated by ordinary least squares regressions of the instantaneous velocities (0.1 s intervals) over a single stride versus the time elapsed (Granatosky, 2016). Trials that involved significant acceleration or deceleration ($\alpha = 0.01$) were excluded. Kinematic and force data were synchronized by resampling 5 % increments of data points during stance, with variables at 21 evenly spaced time points interpolated using the function approxfun() in R (R Core Team, 2020).

Joint coordinate systems for the fore- and hindlimbs followed Sullivan (2007). Three rotational degrees of freedom were considered for the shoulder and hip, whereas only flexion-extension was considered for elbow, wrist, knee, and ankle joints, due to limitations of skin marker-based measurements of limb kinematics. For the shoulder and hip in the reference pose (fore- and hindlimbs fully extended and pointing laterally: Fig. 1A–C), the *x*-axis (pink) points laterally, coincides with the long axis of the humerus and femur, and with rotation about this axis representing their external-internal rotation. The *y*-axis (green) points posteriorly, perpendicular to the *x*- and *z*-axes, with rotation about this axis representing abduction-adduction. The *z*-axis (blue) points ventrally, perpendicular to the *x*- and *y*-axes and in the same plane as the shoulder, elbow, and wrist in the forelimb and the hip, knee, and ankle in the hindlimb (Blob and Biewener, 2001), with rotation about this axis representing retraction-protraction. Joint angles from the reference pose were measured for each of the three rotational axes of the shoulder and hip. The rotation order of the three axes was *z*-*y*-*x*, and the right-hand rule convention (counterclockwise positive and clockwise negative rotation as viewed from the arrow tip) was

used. Long axis rotation was measured using the shoulder, elbow, and wrist landmarks for the humerus in the forelimb, and the hip, knee, and ankle landmarks for the femur in the hindlimb, assuming that elbow and knee abduction-adduction is minimal during stance (Clemente et al., 2011; Irschick and Jayne, 2000). We acknowledge the skin marker-based flexion-extension axes of the elbow, wrist, knee, and ankle could change with respect to osteologically defined joint axes during stance due to abduction-adduction, long axis rotation, and translation about the joints (Manafzadeh and Gatesy, 2021; Manafzadeh et al., 2021; Sullivan, 2007), thus the method we employed should be regarded as providing only approximate kinematic measurements.

Joint moments exerted by the GRF were calculated for each of the rotational axes in the fore- and hindlimbs, based on the GRF vectors and the joint coordinates. The GRF vector was resolved into the directions of two axes perpendicular to each other and to the rotational axis of interest, and then two opposing moments about the rotational axis were summed (Fig. 1D). For example, to calculate the hip abduction-adduction moment, the GRF vector was first resolved into two components parallel to the long axis of the femur (GRF_x) and the hip retraction-protraction axis (GRF_z). Given that moment arms of GRF_x and GRF_z about the rotational axis are R_z and R_x, respectively, the hip abduction-adduction moment is $R_x \times GRF_z - R_z \times GRF_x$ (Fig. 1D). The right-hand rule convention for a positive moment about each rotational axis was used. Because fore- and hindlimb steps sometimes had minor overlap during either the ending of steps for the forelimb or the beginning of stance for the hindlimb, the center of pressure (CoP) of each step was estimated from video. At the beginning of stance, the CoPs were positioned at the metacarpophalangeal and metatarsophalangeal joint landmarks, respectively, because those joints are approximately in the center of the foot contact surfaces. As the fore- and hindfoot start to lift off the ground, the CoPs were constantly moved towards the tip of the digit III until toe-off (Blob and Biewener, 2001). Joint moments calculated here should be interpreted

with caution, because skin markers were displaced from osteological joint centers and would incur some error. We did not measure joint moments from segment inertia and gravity, which might cause some error in calculations of total joint moment, particularly at proximal joints.

The horizontal center of mass (CoM) of each alligator was measured using two balances (Clemente, 2014). A wooden or Plexiglas beam was loaded on two balances, where each end of the beam was supported at the center of each balance. The animals were placed on the beam in a neutral posture (elbow and knee pointing laterally and forearm and lower leg parallel to the body axis), with the snout tip aligned with the end of the beam, and maintained a steady position during measurement. The CoM was represented as a percentage of the shoulder-hip distance (CoM_{SH}), using an equation: $CoM_{SH} = 100[W_2 \times L/(W_1+W_2) - SSL]/(SHL - SSL)$, where L is the length of the beam, SHL is the shoulder-hip length, SSL is the snout-shoulder length, and W_1 and W_2 are the masses recorded at the cranial and caudal balances, respectively. A CoM_{SH} of 0 or 100 would indicate the CoM positioned at the shoulder or hip, respectively.

Data visualization and statistical analyses

A bivariate plot showing the relationship of the limb phase (ratio of the duration between the touchdown of a forelimb and its ipsilateral hindlimb, to the total stride time: modified from Hildebrand, 1976) and duty factor was made to compare gaits among the three size classes of alligators. Only trials where steady-speed fore- and hindlimb steps were filmed in a single video were used for gait comparisons. Speed and stride parameters, joint angles, normalized peak forces, and normalized peak joint moments were compared for fore- and hindlimbs among the three size classes. Speed and stride parameters included 1) dimensionless speed $[u(g \cdot h)^{-0.5}]$, where u is walking speed, g is the acceleration of gravity, and h is the extended hip to ankle length, 2) stride duration, 3) duty factor, and 4) stride length standardized to the total length. The

joint angles compared for each limb were 1) retraction-protraction, 2) adduction, and 3) long axis rotation angles of the humerus and femur, 4) flexion angles of the elbow and knee, and 5) plantarflexion angles of the wrist and ankle. Angles 1 and 3 were compared as excursions (maximum minus minimum angles) and angles 2, 4, and 5 were compared as mean angles during mid-stance (25–75 % of stance). Force parameters compared were 1) peak vertical forces, 2) peak propulsive forces, 3) peak braking forces, 4) peak medial forces normalized to body weight unit, and 5) average GRF medial inclination angles (angles between GRF vectors and the plane including the dorsoventral axis and the direction of travel) during mid-stance. Normalized peak joint moments [$N{\cdot}m/(kg^{4/3})$] compared were 1) shoulder and hip protraction and retraction moments, 2) shoulder and hip abduction moments, 3) humerus and femur external and internal rotation moments, 4) elbow and knee flexion moments, and 5) wrist and ankle dorsiflexion moments. Joint moments ($N{\cdot}m$) were normalized by the 4/3 power of body mass ($kg^{4/3}$) following the convention of human biomechanical studies that use body mass (kg) times a linear dimension (m) such as body height as a normalization factor (Moisio et al., 2003), which scales with $kg^{4/3}$ under the assumption of isometric growth.

Linear mixed effects models were employed to compare the speed, stride, joint angle, force, and peak joint moment variables among the three size classes of alligators, with the size class and dimensionless speed as fixed effects, intercept for individuals as a random effect, and no interaction term, using the package lme4 (Bates et al., 2015) in R v.3.6.3 (R Core Team, 2020). For the comparison of dimensionless speed, only the size class was used as a fixed effect. ANOVA comparing the full model and the reduced model without the size class as a fixed effect was conducted to test for a significant effect of size class ($\alpha = 0.05$), and the effect size Ω^2 (Xu, 2003) was calculated using the R package performance (Lüdecke et al., 2020). Additionally, post-hoc pairwise comparisons of all size class pairs were performed using the R package

multcomp (α = 0.05) (Hothorn et al., 2008). Comparisons were visually aided by line plots of joint angles, ground reaction forces, and joint moments. To evaluate degrees of overall fore- and hindlimb flexion, shoulder and hip height profiles during stance were also calculated. Walking trials where the shoulder and hip heights at touchdown and toe-off differed by more than 10 % were excluded. Line plots were created using 5 % increments of data points during stance.

RESULTS

Seven alligators from three size classes (three small, three medium, and one large) performed steady speed walks, and 73 forelimb strides (32, 25, and 16 strides for small, medium, and large classes, respectively) and 63 hindlimb strides (22, 21, and 20 strides for small, medium, and large classes, respectively) were recorded. Alligators chose gaits that included walking trots and diagonal couplet walks (Hildebrand, 1976) irrespective of the size classes, with limb phases of 0.43–0.59 (Fig. S1). No aerial phase was observed in any trial.

Dimensionless speed was faster in smaller classes, and stride duration was longer in the large class than the small and medium classes for fore- and hindlimbs (Table 1). Duty factor was not significantly different among size classes in the forelimb, while it was higher in the large class than the small class in the hindlimb (Table 1). The minimum duty factor was lower in smaller size classes in the forelimb (0.56, 0.61, and 0.67 for small, medium, and large classes) and the hindlimb (0.63, 0.70, and 0.76 for small, medium, and large classes). Normalized stride lengths were longer in the small size class: significant differences were found between the small and medium classes in fore- and hindlimbs (Table 1).

Limb joint angles during mid-stance were also size-dependent in alligators (Fig. 2). All angles, except humerus and femur retraction-protraction, elbow flexion, and wrist plantarflexion angles, showed some differences between size classes (Table 2). The humerus and femur were more adducted in the medium and large classes than in the small class, as pairwise comparisons showed significant or nearly significant differences between these larger classes and the small class (Fig. 3A–C,G–I, Table 2). Degrees of humeral axial rotation were larger in the small class than in the large and medium classes, whereas those of femoral rotation were larger in the medium class than in the small and large classes (Fig. 3A–C,G–I, Table 2). The knee and ankle were less flexed in the medium and large classes than in the small class (Fig. 3J–L, Table 2). More abducted shoulder and hip and flexed knee and ankle in the small class were reflected in its lower shoulder and hip height profiles (Fig. 3M–O). The shoulder and hip height profiles overlapped during stance in the small class, whereas the hip was higher than the shoulder during stance in the medium and large classes.

The fore- and hindlimbs were primarily used for braking and propulsion, respectively, while both fore- and hindlimbs produced medial forces during stance. Comparisons of normalized peak forces showed that peak vertical forces of the forelimb were larger in the small class than the medium and large classes, whereas those of the hindlimb were larger in the medium and large classes than the small class (Fig. 4, Table 3). Peak propulsive, braking, and medial forces in the forelimb were smaller in the medium size class than the small class (Fig. 4, Table 3). No significant difference among size classes was found for the hindlimb peak propulsive, braking, and medial forces. GRF was directed nearly vertically at midstance for both limbs and all size classes (Table 3). Medial inclination of the GRF at mid-stance was similar across the size classes for the forelimb, averaging about 8–9°. For the hindlimb, medial inclination of the GRF varied

slightly more across size classes with smaller individuals showing more inclined forces than larger ones, but still averaging only 7–11° across the groups.

Shoulder protraction and abduction, humerus external rotation, elbow flexion, and wrist dorsiflexion moments dominated for the forelimb, and hip retraction and abduction, knee flexion, and ankle dorsiflexion moments dominated for the hindlimb during stance (Fig. 5). Comparisons of normalized peak joint moments showed that peak shoulder protraction and abduction moments were generally larger in the small class than the medium and large classes, and peak hip retraction and abduction moments were larger in the small class than the medium class (Fig. 5A–C,G–I, Table 4). Peak humeral and femoral internal rotation moments were smaller in the medium class than either the small or large class (Table 4). Peak elbow flexion moments were larger in the small and large classes than the medium class, and peak knee flexion moments were larger in the large class than the small and medium classes (Fig. 5D–F,J–L, Table 4). No significant difference among size classes was found for humeral and femoral external rotation moments or wrist and ankle dorsiflexion moments (Table 4). Sensitivity analyses of peak fore- and hindlimb joint moments using either the dorsal, ventral, anterior, or posterior edge of each fore- and hindlimb joint landmark (3.4–9.3 mm diameter) in a representative trial (al09f21) showed that landmark-dependent errors for dominant joint moments [>0.05 $N{\cdot}m/(kg^{4/3})$] averaged less than 20% from the original estimates that used the center of each landmark (Table S1), providing confidence that the patterns we identified are robust to digitizing error from marker placement or skin motion over a joint.

The CoM shifts from juveniles through subadults in alligators. CoM is positioned in the mid-torso (CoM_{SH} 57–62 %) in the small class (0.23–0.26 kg), moves posteriorly near the hip (CoM_{SH} 65–80 %) in the medium class (0.68–2.80 kg), and then moves back anteriorly (CoM_{SH} 64–72 %) in the large class (3.71–8.00 kg) (Fig. 6A).

DISCUSSION

Larger alligators walked slowly with longer stride durations. Mean duty factors did not differ significantly across size classes, except between small and large animals for the hindlimb (Table 1); however, the minimum duty factor was higher in larger size classes for fore- and hindlimbs (see the results). Slower movement of larger alligators would allow them to distribute forces over a longer stance duration, and reduce peak muscle and bone stresses (Alexander et al., 1979b; Dick and Clemente, 2017).

Ontogenetic changes in limb posture and their mechanical consequences

Comparisons of limb posture among juvenile to subadult alligators revealed that larger size classes use a more adducted humerus and femur, a less flexed knee, and a less dorsiflexed ankle than the small class (Figs 2,3; Table 2). The ontogenetic shift from more sprawled and crouched posture to more upright posture in alligators is comparable to the interspecific trend in quadrupedal mammals—larger mammals use more upright limb posture than smaller ones at the speed of the trot-gallop transition (Biewener, 1989, 1990). Consequently, fore- and hindlimb muscle EMA (ratio of the muscle moment arm to the GRF moment arm) in large mammals is higher than that in smaller ones with more crouched limb posture (Biewener, 1989, 1990). Positive scaling of limb muscle EMA against mass has been observed in phylogenetically diverse lineages, and similar scaling relationships have been found among more restricted groups (i.e., cercopithecine primates and rodents: Biewener, 2005; Polk, 2002). Notable exceptions to the mammalian trend are felids, where limb posture does not largely change across a 50-fold range in mass (Day and Jayne, 2007). However, the EMA of the elbow and knee extensors may scale positively among felids due to positive scaling of the muscle moment arms (Harper and Sylvester, 2019), which requires further testing. Overall positive scaling of the limb muscle EMA in

mammals allows them to keep up with the demands for muscle force production while maintaining muscle and bone stresses over a range of mass, though large erect animals may sacrifice a cost in acceleration and maneuverability (Biewener, 1989; Biewener, 1990; Cuff et al., 2016; Gray, 1968). In contrast to quadrupedal mammals with parasagittal limb posture, varanid lizards with non-parasagittal limb posture do not appear to change hindlimb posture during running over a size range of 0.04–7.9 kg (Clemente et al., 2011). Conceivably, hindlimb muscle EMA may decrease with more upright posture in varanids, and they may reduce limb bone stresses by minimizing internal rotation of the femur at mid-stance (Clemente et al., 2011).

The similarity of postural shifts during ontogeny in alligators and across mass in mammals, but not varanids, is not easy to explain. Counterintuitively, *in vivo* and theoretical studies indicated that hindlimb bone stresses increase as individual American alligators select the use of more upright hindlimb posture (Blob and Biewener, 1999, 2001). During the use of more upright stance by animals in a size range between the medium and large animals of the current study, an anterior shift in the CoP of the hindfoot increased the moment arm of the GRF about the ankle (Blob and Biewener, 2001). This increased ankle flexion moment was hypothesized to be countered by a chain of increased muscle activation and force production spanning from the ankle extensors that cross the ankle and knee joints to the knee extensor muscles, inducing higher dorsoventral bending stress in the femur (Blob and Biewener, 2001; Reilly and Blob, 2003). Comparisons of electromyographic burst intensities of stance phase muscles at different femoral adduction angles revealed more intense bursts of ankle and knee extensors during more upright steps, supporting the chain of muscle activation hypothesis (Reilly and Blob, 2003). However, our ontogenetic comparisons of limb posture and joint moments in alligators did not provide a simple parallel to the patterns from these previous observations of postural change by medium-sized individuals. Although hindlimb posture was more upright in the medium and large

classes than the small class, normalized ankle and knee flexion moments were not different among size classes, except the larger knee flexion moment of the large class compared to other classes (Table 4). To better understand the differences between these analyses, we took the separate data from each individual alligator in this study and conducted a least squares regression of ankle dorsiflexion moment on femoral adduction angle. Interpretations should be made cautiously given our small sample sizes of trials for some individuals; however, within each individual alligator, more adducted (upright) femoral postures also showed greater ankle dorsiflexion moments, with regressions indicating significant or nearly significant correlations for two of seven individuals (Table S2). These results further suggest that the consequences of postural change within an animal at a particular body size may differ from consequences of postural change compared across different body sizes.

Differing impacts of postural change across gradients of body size are likely related to allometric growth of body and limb proportions and their consequences for joint moments among size classes. Based on the measurement datasets of Farlow et al. (2005) and Iijima and Kubo (2019), length percentages of the femur to the hindlimb (sum of the femur, tibia, and metatarsal III) would be 35.8, 40.4, and 42.6%, respectively, and those of the hindlimb to presacral vertebrae would be 72.0, 66.6, and 63.0%, for the average sizes of the small, medium, and large classes, respectively. Due to the shorter hindlimb and distal segments (tibia and metatarsal III) within the hindlimb, larger alligators might incur smaller normalized joint moments about the ankle and knee. Therefore, the chain activation of the ankle and knee flexors (Blob and Biewener, 2001; Reilly and Blob, 2003) would be mitigated in larger alligators.

The use of more upright limb posture in larger alligators could have mechanical benefits in the context of the muscle forces exerted in the fore- and hindlimbs. Limb muscle masses and cross-sectional areas generally scale with overall geometric similarity in American alligators

(Allen et al., 2010), so it would be increasingly challenging for larger alligators to support their weights unless changes in limb posture or proportions allow them to reduce joint moments. Indeed, larger alligators used more adducted fore- and hindlimb posture, and their normalized shoulder and hip abduction moments were reduced, which would be expected to require lower levels of recruitment for shoulder and hip adductor muscles during stance (Figs 3,5; Tables 2,4). Furthermore, large individuals of other crocodylian species also commonly walk with upright limb posture (Cott, 1961; Farlow et al., 2018) with the exception of Indian gharials, the most aquatic extant crocodylians that possess considerably shortened limbs (Bustard and Singh, 1977; Iijima et al., 2018; Singh and Bustard, 1976).

Ontogenetic changes in limb posture have been observed in some species of mammals and lizards. Domestic cats and Vervet monkeys show more flexed limbs in the first few weeks after birth due to their immature neuromuscular system and lack of stability (Howland et al., 1995; Peters, 1983; Vilensky and Gankiewicz, 1989). Similarly, fore- and hindlimbs of certain dog breeds (e.g. beagles), and the hindlimbs of horses, become slightly more erect as juveniles grow to adult size (Grossi and Canals, 2010; Helmsmüller et al., 2014). Other studies have highlighted various ontogenetic trends in fore- and hindlimb joint angles that are associated with changes in limb proportions, CoM, limb force distribution, and limb function, as well as mass (Burgess et al., 2016; Patel et al., 2013; Young, 2009, 2012; Young and Shapiro, 2018; Zeininger et al., 2017). As for lizards, desert iguanas change limb posture through ontogeny, where adults use more crouched posture than juveniles at the speed of the walk-run transition (Irschick and Jayne, 2000). However, more extended limb posture in juvenile desert iguanas might be explained by their significantly longer limbs as compared to adults (Irschick and Jayne, 2000), which would increase joint moments if the same limb joint angles were used as in adults (Polk, 2002). In American alligators, the smallest individuals that we examined showed steady and stable steps;

thus, an underdeveloped neuromuscular system should not be the cause of their flexed limb posture. Moreover, alligators show negative scaling of hindlimb length against trunk length as in desert iguanas, but the scaling exponent is closer to one and allometric morphological changes are smaller (Dodson, 1975; Farlow and Britton, 2000; Iijima and Kubo, 2019).

Ontogenetic changes in limb posture in alligators involve alterations of not only humerus and femur adduction and the knee and ankle flexion angles, but also degrees of humerus and femur long axis rotation during stance. In the forelimb, the medium and large classes that use a more adducted humerus also showed smaller degrees of humeral axial rotation than the small size class, due to lesser external rotation at the touchdown of the manus and lesser internal rotation at its lift-off (Fig. 3A–C, Table 2). Meanwhile, in the hindlimb, the medium and large size classes that walked with a more adducted femur showed greater degrees of femoral axial rotation than the small class due to lesser internal rotation at foot touchdown (Fig. 3G–I, Table 2). Previous studies of fore- and hindlimb kinematics in sprawling to erect quadrupeds, including salamanders, lizards, crocodylians, opossums, and rats, have suggested such an association between greater adduction and lesser degrees of humerus and femur axial rotation during stance (Baier and Gatesy, 2013; Bakker, 1971; Bonnan et al., 2016; Gatesy, 1991; Irschick and Jayne, 1999; Jenkins, 1971; Karakasiliotis et al., 2013; Nyakatura et al., 2014, 2019; Sullivan, 2007). The association of greater humeral adduction and lesser humeral axial rotation in alligators matches expectations from other taxa, but the finding of greater femoral adduction and greater femoral axial rotation was unexpected. Even with more erect limb posture, internal rotation of the femur may play an important role during stance in alligators, given the potential for a strong internal rotation moment about the femoral long axis exerted by the femoral retractor M. caudofemoralis longus (CFL) (Blob, 2000; Gatesy, 1990; Gatesy, 1997; Reilly et al., 2005). However, some

debate about this possibility also exists, as CFL has been regarded as an external rotator of the femur in some recent studies of crocodylians (Allen et al., 2021; Wiseman et al., 2021).

Ontogenetic changes in the CoM and limb force distribution

Additional intriguing aspects of locomotor ontogeny in alligators besides postural shifts are changes in the CoM and fore- and hindlimb force distribution. The CoM is positioned more anteriorly in small individuals (Fig. 6A). During ontogeny, the CoM shifts backward from the small (0.23–0.26 kg) through medium (0.68–2.80 kg) classes, and then shifts slightly forward from the medium (0.68–2.80 kg) through large (3.71–8.00 kg) classes. The more anteriorly positioned CoM in the small class coincided with their higher forelimb and lower hindlimb normalized peak vertical forces as compared to larger classes (Fig. 4, Table 3). Nonetheless, division of labor was maintained throughout the size classes, where fore- and hindlimbs produced net braking and propulsive forces, respectively (Fig. 4).

Limb force distribution varies among quadrupeds. In mammals, peak vertical forces are forelimb dominant in non-primates including rats, cats, horses, giraffes, bears, and elephants (Basu et al., 2019; Granatosky et al., 2018; Merkens et al., 1985; Ren et al., 2010; Shine et al., 2015; Zumwalt et al., 2006), but hindlimb dominant in most primates (Demes et al., 1994; Kimura et al., 1979). It should also be noted that peak forces and impulses become increasingly hindlimb dominant with higher running speeds in some cursorial mammals (Hudson et al., 2012; Self Davies et al., 2019). Among amphibians and reptiles, vertical forces are potentially forelimb dominant in subadult spectacled caimans (Nyakatura et al., 2019), hindlimb dominant in varanid lizards and juvenile American alligators (Cieri et al., 2021; Willey et al., 2004), evenly distributed between fore- and hindlimbs in Indo-Pacific geckos (Chen et al., 2006), and exhibit various patterns across salamanders and multiple lizard families (Kawano et al., 2016; McElroy

et al., 2014; Nyakatura et al., 2019). Limb force distribution also varies intraspecifically. Decreases in relative fore- vs. hindlimb peak vertical forces, together with the caudal shift of the CoM, occur during ontogeny in primates (Druelle et al., 2017; Grand, 1983; Turnquist and Wells, 1994; Young, 2012). In contrast, forelimbs become more dominant weight supporters during postnatal weeks 11–51 in dogs such as beagles, because more retracted forelimbs place the forefeet closer to the CoM, and abdominal organs grow with negative allometry (Helmsmüller et al., 2014). However, in a different breed of dogs, relative fore- vs. hindlimb peak vertical forces decreased during postnatal weeks 4–15, but remained unchanged in adults (Biknevicius et al., 1997). Furthermore, interspecific allometry of limb force distribution was reported in varanid lizards, where allometric exponents of peak vertical forces and vertical impulses were larger for hindlimbs than forelimbs, and the CoM was more caudally positioned in larger species (Cieri et al., 2021).

Forelimb dominance of peak vertical forces in small alligators is explained by not only their more anteriorly positioned CoM, but also their compliant hindlimbs. In small alligators, stance phase was characterized by more flexed hindlimbs than forelimbs, and by smaller vertical oscillation of the hip than the shoulder. Compliant walking is known to lengthen stance duration, flatten the profile and reduce the peaks of vertical forces, but increase mechanical cost (McMahon et al., 1987; Ren et al., 2010; Schmitt, 1999; Schmitt and Hanna, 2004; Young, 2012). Additionally, though we did not examine whole-body mechanics, more compliant hindlimbs in small alligators are expected to reduce energy recovery through the inverted pendulum mechanism (Willey et al., 2004). Given these disadvantages, reasons as to why small alligators (total length ~0.5 m, body mass ~0.3 kg) walk with compliant hindlimbs remains uncertain. One possibility (suggested by a reviewer of this manuscript) could be that using more flexed hindlimbs may allow the hindlimb extensor muscles to operate at longer fascicle lengths that could

improve their shortening velocity and capacity for mechanical work. Such advantages for mechanical power generation in the hindlimbs could be significant for smaller alligators, which likely face a greater risk of predation and could benefit from accelerating their body away from threats.

The anterior shift of the CoM from the medium (0.68–2.80 kg) through large (3.71–8.00 kg) classes most likely continues through adult size in alligators due to the allometric growth of their body segments. In American alligators, many of the jaw adductor muscle masses scale with positive allometry against snout-vent lengths, which enables positive scaling of bite force (Erickson et al., 2003; Gignac and Erickson, 2016). Furthermore, in non-gavialid crocodylians including American alligators, forelimbs grow faster than hindlimbs; thus, larger individuals have increasingly longer and thicker forelimb bones (Iijima and Kubo, 2019: Fig. 6B). A relatively heavier head and forelimbs would together place the CoM more anteriorly in larger alligators, which is in accord with the craniodorsal CoM shift in juvenile to adult freshwater crocodiles estimated by computational modeling (Allen et al., 2009). Future studies of terrestrial locomotion among full-size adult alligators could give further insights into how animals with non-parasagittal limb posture modulate limb joint angles, joint moments, and limb force distribution as they increase masses and change in body proportions and inertial properties. Such empirical data on size-dependent changes in the locomotion of crocodylians could provide a basis for discussing the evolution of body size and erect limb posture in early archosauriforms.

Acknowledgments

The authors thank D. LeJeune and M. Miller (Louisiana Department of Wildlife and Fisheries) for assistance with sampling alligators, and M. Hart (South Carolina Department of Natural Resources), R. Flynt (Mississippi Department of Wildlife, Parks and Fisheries), C. Threadgill

and T. Ancelet (Alabama Department of Conservation and Natural Resources), and J. Hawkins (Georgia Department of Natural Resources) for permissions to transport and house alligators. We also thank K. Diamond, C. Kinsey, A. Palecek, and D. Adams for assistance with experiments, M. Novak, G. Griner, N. Greenslit, N. Schneider, C. Tresslar, A. J. McKamy, C. Ollis, A-M. Riley, and K. Miles for help with animal care, S. Fujiwara, J. Hutchinson, and C. Mayerl for inputs and discussions, and two anonymous reviewers for their helpful comments.

Competing interests

The authors declare no competing financial, professional, or personal interests.

Author contributions

M.I. and R.W.B. designed the experiments. M.I., V.D.M. and R.W.B. ran the experiments. M.I. wrote R scripts and analyzed the data. M.I., V.D.M., R.M.E. and R.W.B. contributed to interpreting the results, writing the manuscript, and approving all drafts of the manuscript.

Funding

This work was supported by JSPS Grant-in-Aid for Scientific Research [19J00701 to M.I.].

Data availability

Data upon which analyses are based are available from the figshare repository. DOI: 10.6084/m9.figshare.16669747

References

Alexander, R. M., Jayes, A. S., Maloiy, G. M. O. and Wathuta, E. M. (1979a). Allometry of the limb bones of mammals from shrews (*Sorex*) to elephant (*Loxodonta*). *J. Zool.* **189**, 305–314.

Alexander, R. M., Maloiy, G. M. O., Hunter, B., Jayes, A. S. and Nturibi, J. (1979b). Mechanical stresses in fast locomotion of buffalo (*Syncerus caffer*) and elephant (*Loxodonta africana*). *J. Zool.* **189**, 135–144.

Alexander, R. M., Jayes, A. S., Maloiy, G. M. O. and Wathuta, E. M. (1981). Allometry of the leg muscles of mammals. *J. Zool.* **194**, 539–552.

Allen, V., Paxton, H. and Hutchinson, J. R. (2009). Variation in center of mass estimates for extant sauropsids and its importance for reconstructing inertial properties of extinct archosaurs. *Anat. Rec.* **292**, 1442–1461.

Allen, V., Elsey, R. M., Jones, N., Wright, J. and Hutchinson, J. R. (2010). Functional specialization and ontogenetic scaling of limb anatomy in *Alligator mississippiensis*. *J. Anat.* **216**, 423–445.

Allen, V. R., Kilbourne, B. M. and Hutchinson, J. R. (2021). The evolution of pelvic limb muscle moment arms in bird-line archosaurs. *Sci. Adv.* 7, eabe2778.

Baier, D. B. and Gatesy, S. M. (2013). Three-dimensional skeletal kinematics of the shoulder girdle and forelimb in walking *Alligator*. *J. Anat.* **223**, 462–473.

Bakker, R. (1971). Dinosaur physiology and the origin of mammals. *Evolution* **25**, 636–658.

Basu, C., Wilson, A. M. and Hutchinson, J. R. (2019). The locomotor kinematics and ground reaction forces of walking giraffes. *J. Exp. Biol.* **222**, 159277.

Bates, D., Mächler, M., Bolker, B. M. and Walker, S. C. (2015). Fitting linear mixed-effects models using lme4. *J. Stat. Softw.* **67**, 1–48.

Benton, M. J. and Clark, J. M. (1988). Archosaur phylogeny and the relationships of the Crocodylia. In *The Phylogeny and Classification of the Tetrapods, vol. 1* (ed. Benton, M. J.), pp. 295–338. Oxford: Clarendon Press.

Bertram, J. E. A. and Biewener, A. A. (1990). Differential scaling of the long bones in the terrestrial Carnivora and other mammals. *J. Morphol.* **204**, 157–169.

Biewener, A. A. (1983). Allometry of quadrupedal locomotion: the scaling of duty factor, bone curvature and limb orientation to body size. *J. Exp. Biol.* **105**, 147–171.

Biewener, A. A. (1989). Scaling body support in mammals: limb posture and muscle mechanics. *Science* **245**, 45–48.

Biewener, A. A. (1990). Biomechanics of mammalian terrestrial locomotion. *Science* **250**, 1097–1103.

Biewener, A. A. (2005). Biomechanical consequences of scaling. *J. Exp. Biol.* **208**, 1665–1676.

Biewener, A. A. (2015). Going from small to large: mechanical implications of body size diversity in terrestrial mammals. In *Great Transformations in Vertebrate Evolution* (eds. Dial, K. P., Shubin, N., and Brainerd, E. L.), pp. 227–238. Chicago: University of Chicago Press.

Biewener, A. A. and Patek, S. N. (2018). *Animal Locomotion*. New York: Oxford University Press.

Biknevicius, A. R., Heinrich, R. E. and Dankoski, E. (1997). Effects of ontogeny on locomotor kinetics. *J. Morphol.* **232 (ICVM-5 Abstract)**, 235.

Blob, R. W. (2000). Interspecific scaling of the hindlimb skeleton in lizards, crocodilians, felids and canids: does limb bone shape correlate with limb posture? *J. Zool.* **250**, 507–531.

Blob, R. W. and Biewener, A. A. (1999). In vivo locomotor strain in the hindlimb bones of *Alligator mississippiensis* and *Iguana iguana*: implications for the evolution of limb bone safety factor and non-sprawling limb posture. *J. Exp. Biol.* **202**, 1023–1046.

Blob, R. W. and Biewener, A. A. (2001). Mechanics of limb bone loading during terrestrial locomotion in the green iguana (*Iguana iguana*) and American alligator (*Alligator mississippiensis*). *J. Exp. Biol.* **204**, 1099–1122.

Bonaparte, J. F. (1984). Locomotion in rauisuchid thecodonts. *J. Vertebr. Paleontol.* **3**, 210–218.

Bonnan, M. F., Shulman, J., Varadharajan, R., Gilbert, C., Wilkes, M., Horner, A. and Brainerd, E. (2016). Forelimb kinematics of rats using XROMM, with implications for small eutherians and their fossil relatives. *PLoS ONE* **11**, 1–21.

Brinkman, D. (1980). The hind limb step cycle of *Caiman sclerops* and the mechanics of the crocodile tarsus and metatarsus. *Can. J. Zool.* **58**, 2187–2200.

Burgess, M. L., Schmitt, D., Zeininger, A., McFarlin, S. C., Zihlman, A. L., Polk, J. D. and Ruff, C. B. (2016). Ontogenetic scaling of fore limb and hind limb joint posture and limb bone cross-sectional geometry in vervets and baboons. *Am. J. Phys. Anthropol.* **161**, 72–83.

Bustard, H. R. and Singh, L. A. K. (1977). Studies on the Indian gharial *Gavialis gangeticus* (Gmelin) (Reptilia, Crocodilia): change in terrestrial locomotory pattern with age. *J. Bombay Nat. Hist. Soc.* **74**, 534–537.

Butcher, M. T., and Blob, R. W. (2008). Mechanics of limb bone loading during terrestrial locomotion in river cooter turtles (*Pseudemys concinna*). *J. Exp. Biol.* **211**, 1187–1202.

Campione, N. E. and Evans, D. C. (2012). A universal scaling relationship between body mass and proximal limb bone dimensions in quadrupedal terrestrial tetrapods. *BMC Biol.* **10**, doi:10.1186/1741-7007-10-60.

Charig, A. J. (1972). The evolution of the archosaur pelvis and hindlimb: an explanation in functional terms. In *Studies in Vertebrate Evolution* (eds. Joysey, K. A. and Kemp, T. S.), pp. 121–155. Edinburgh: Oliver and Boyd.

Chen, J. J., Peattie, A. M., Autumn, K. and Full, R. J. (2006). Differential leg function in a sprawled-posture quadrupedal trotter. *J. Exp. Biol.* **209**, 249–259.

Christian, A. and Garland, T. (1996). Scaling of limb proportions in monitor lizards (Squamata: Varanidae). *J. Herpetol.* **30**, 219–230.

Cieri, R. L., Dick, T. J. M. and Clemente, C. J. (2020). Monitoring muscle over three orders of magnitude: widespread positive allometry among locomotor and body support musculature in the pectoral girdle of varanid lizards (Varanidae). *J. Anat.* **237**, 1114–1135.

Cieri, R. L., Dick, T. J. M., Irwin, R., Rumsey, D. and Clemente, C. J. (2021). The scaling of ground reaction forces and duty factor in monitor lizards: implications for locomotion in sprawling tetrapods. *Biol. Lett.* **17**, 20200612.

Clemente, C. J. (2014). The evolution of bipedal running in lizards suggests a consequential origin may be exploited in later lineages. *Evolution* **68**, 2171–2183.

Clemente, C. J., Withers, P. C., Thompson, G. and Lloyd, D. (2011). Evolution of limb bone loading and body size in varanid lizards. *J. Exp. Biol.* **214**, 3013–3020.

Clemente, C. J., Withers, P. C. and Thompson, G. (2012). Optimal body size with respect to maximal speed for the yellow-spotted monitor lizard (*Varanus panoptes*; Varanidae). *Physiol. Biochem. Zool.* **85**, 265–273.

Cott, H. B. (1961). Scientific results of an inquiry into the ecology and economic status of the Nile Crocodile (*Crocodilus niloticus*) in Uganda and Northern Rhodesia. *Trans. Zool. Soc. London* **29**, 211–356.

Cuff, A. R., Sparkes, E. L., Randau, M., Pierce, S. E., Kitchener, A. C., Goswami, A. and Hutchinson, J. R. (2016). The scaling of postcranial muscles in cats (Felidae) II: hindlimb and lumbosacral muscles. *J. Anat.* **229**, 142–152.

Daley, M. A. and Birn-Jeffery, A. (2018). Scaling of avian bipedal locomotion reveals independent effects of body mass and leg posture on gait. *J. Exp. Biol.* **221**, jeb152538.

Day, L. M. and Jayne, B. C. (2007). Interspecific scaling of the morphology and posture of the limbs during the locomotion of cats (Felidae). *J. Exp. Biol.* **210**, 642–654.

Demes, B., Larson, S. G., Stern, J. T., Jungers, W. L., Biknevicius, A. R. and Schmitt, D. (1994). The kinetics of primate quadrupedalism: "hindlimb drive" reconsidered. *J. Hum. Evol.* **26**, 353–374.

Dick, T. J. M. and Clemente, C. J. (2017). Where have all the giants gone? How animals deal with the problem of size. *PLoS Biol.* **15**, e2000473.

Dodson, P. (1975). Functional and ecological significance of relative growth in *Alligator*. *J. Zool. London* **175**, 315–355.

Druelle, F., Aerts, P., D'Août, K., Moulin, V. and Berillon, G. (2017). Segmental morphometrics of the olive baboon (*Papio anubis*): a longitudinal study from birth to adulthood. *J. Anat.* **230**, 805–819.

Erickson, G. M., Lappin, A. K. and Vliet, K. A. (2003). The ontogeny of bite-force performance in American alligator (*Alligator mississippiensis*). *J. Zool.* **260**, 317–327.

Farlow, J. O. and Britton, A. (2000). Size and body proportions in *Alligator mississippiensis*: implications for archosaurian ichnology. *Paleontol. Soc. Korea Spec. Publ.* **4**, 189–206.

Farlow, J. O., Hurlburt, G. R., Elsey, R. M., Britton, A. R. C. and Langston, W. J. (2005). Femoral dimensions and body size of *Alligator mississippiensis*: estimating the size of extinct mesoeucrocodylians. *J. Vertebr. Paleontol.* **25**, 354–369.

Farlow, J. O., Robinson, N. J., Kumagai, C. J., Paladino, F. V, Falkingham, P. L., Elsey, R. M. and Martin, A. J. (2018). Trackways of the American crocodile (*Crocodylus acutus*) in northwestern Costa Rica: implications for crocodylian ichnology. *Ichnos* **25**, 30–65.

Gatesy, S. M. (1990). Caudefemoral musculature and the evolution of theropod locomotion. *Paleobiology* **16**, 170–186.

Gatesy, S. M. (1991). Hind limb movements of the American alligator (*Alligator mississippiensis*) and postural grades. *J. Zool.* **224**, 577–588.

Gatesy, S. M. (1997). An electromyographic analysis of hindlimb function in *Alligator* during terrestrial locomotion. *J. Morphol.* **234**, 197–212.

Gatesy, S. M. and Biewener, A. A. (1991). Bipedal locomotion: effects of speed, size and limb posture in birds and humans. *J. Zool.* **224**, 127–147.

Gignac, P. M. and Erickson, G. M. (2016). Ontogenetic bite-force modeling of *Alligator mississippiensis*: implications for dietary transitions in a large-bodied vertebrate and the evolution of crocodylian feeding. *J. Zool.* **299**, 229–238.

Granatosky, M. C. (2016). A mechanical analysis of suspensory locomotion in primates and other mammals. Ph.D. dissertation, Duke University, Durham. 443 pp.

Granatosky, M. C., Fitzsimons, A., Zeininger, A. and Schmitt, D. (2018). Mechanisms for the functional differentiation of the propulsive and braking roles of the forelimbs and hindlimbs during quadrupedal walking in primates and felines. *J. Exp. Biol.* **221**, 162917.

Grand, T. I. (1983). The anatomy of growth and its relation to locomotor capacity in Macaca. In *Advances in the Study of Mammalian Behavior* (eds. Eisenberg, J. F. and Kleiman, D. G.), pp. 5–23. Shippensburg: American Society of Mammalogists.

Gray, J. (1968). *Animal Locomotion*. New York: W. W. Norton & Company.

Gregory, W. K. (1912). Notes on the principles of quadrupedal locomotion and on the mechanism of the limbs in hoofed animals. *Ann. N. Y. Acad. Sci.* **22**, 267–294.

Grossi, B. and Canals, M. (2010). Comparison of the morphology of the limbs of juvenile and adult horses (*Equus caballus*) and their implications on the locomotor biomechanics. *J. Exp. Zool. Part A Ecol. Genet. Physiol.* **313 A**, 292–300.

Harper, C. M. and Sylvester, A. D. (2019). Effective mechanical advantage allometry of felid elbow and knee extensors. *Anat. Rec.* **302**, 775–784.

Hedrick, T. L. (2008). Software techniques for two- and three-dimensional kinematic measurements of biological and biomimetic systems. *Bioinspiration and Biomimetics* **3**, 034001.

Heglund, N. C. and Taylor, C. R. (1988). Speed, stride frequency and energy cost per stride: how do they change with body size and gait? *J. Exp. Biol.* **138**, 301–318.

Helmsmüller, D., Anders, A., Nolte, I. and Schilling, N. (2014). Ontogenetic change of the weight support pattern in growing dogs. *J. Exp. Zool. Part A Ecol. Genet. Physiol.* **321**, 254–264.

Hildebrand, M. (1976). Analysis of tetrapod gaits: general considerations and symmetrical gaits. In *Neural Control of Locomotion* (eds. Herman, R. M., Grillner, S., Stei, P. S. G., and Stuart, D. G.), pp. 203–236. New York: Plenum Press.

Hothorn, T., Bretz, F. and Westfall, P. (2008). Simultaneous inference in general parametric models. *Biometrical J.* **50**, 346–363.

Howland, D. R., Bregman, B. S. and Goldberger, M. E. (1995). The development of quadrupedal locomotion in the kitten. *Exp. Neurol.* **135**, 93–107.

Hudson, P. E., Corr, S. A. and Wilson, A. M. (2012). High speed galloping in the cheetah (*Acinonyx jubatus*) and the racing greyhound (*Canis familiaris*): spatio-temporal and kinetic characteristics. *J. Exp. Biol.* **215**, 2425–2434.

Hutchinson, J. R., Felkler, D., Houston, K., Chang, Y. M., Brueggen, J., Kledzik, D. and Vliet, K. A. (2019). Divergent evolution of terrestrial locomotor abilities in extant Crocodylia. *Sci. Rep.* 9, 19302.

Iijima, M. and Kubo, T. (2019). Allometric growth of limb and body proportions in crocodylians. *J. Zool.* **309**, 200–211.

Iijima, M., Kubo, T. and Kobayashi, Y. (2018). Comparative limb proportions reveal differential locomotor morphofunctions of alligatoroids and crocodyloids. *R. Soc. Open Sci.* **5**, 171774.

Irschick, D. J. and Jayne, B. C. (1999). Comparative three-dimensional kinematics of the hindlimb for high-speed bipedal and quadrupedal locomotion of lizards. *J. Exp. Biol.* **202**, 1047–1065.

Irschick, D. J. and Jayne, B. C. (2000). Size matters: ontogenetic variation in the three-dimensional kinematics of steady-speed locomotion in the lizard *Dipsosaurus dorsalis*. *J. Exp. Biol.* **203**, 2133–2148.

Jenkins, F. A. (1971). Limb posture and locomotion in the Virginia opossum (*Didelphis marsupialis*) and in other non- cursorial mammals. *J. Zool.* **165**, 303–315.

Karakasiliotis, K., Schilling, N., Cabelguen, J. M. and Ijspeert, A. J. (2013). Where are we in understanding salamander locomotion: biological and robotic perspectives on kinematics. *Biol. Cybern.* **107**, 529–544.

Kawano, S. M., Economy, D. R., Kennedy, M. S., Dean, D. and Blob, R. W. (2016). Comparative limb bone loading in the humerus and femur of the tiger salamander: testing the “mixed-chain” hypothesis for skeletal safety factors. *J. Exp. Biol.* **219**, 341–353.

Kimura, T., Okada, M. and Ishida, H. (1979). Kinesiological characteristics of primate walking: its significance in human walking. In *Environment, Behavior and Morphology: Dynamic Interactions in Primates* (eds. Morbeck, M. E., Preuschoft, H., and Gomberg, N.), p. 297–311. New York: G. Fischer.

Kram, R. and Taylor, C. R. (1990). Energetics of running: a new perspective. *Nature* **346**, 265–267.

Lüdecke, D., Makowski, D., Waggoner, P., Patil, I. and Ben-Shachar, M. S. (2020). Assessment of regression models performance. *CRAN*. doi:10.5281/zenodo.3952174

Manafzadeh, A. R. and Gatesy, S. M. (2021). Paleobiological reconstructions of articular function require all six degrees of freedom. *J. Anat.* doi:10.1111/joa.13513

Manafzadeh, A. R., Kambic, R. E. and Gatesy, S. M. (2021). A new role for joint mobility in reconstructing vertebrate locomotor evolution. *Proc. Natl. Acad. Sci.* **118**, e2023513118.

McElroy, E. J., Wilson, R., Biknevicius, A. R. and Reilly, S. M. (2014). A comparative study of single-leg ground reaction forces in running lizards. *J. Exp. Biol.* **217**, 735–742.

McMahon, T. (1973). Size and shape in biology. *Science* **179**, 1201–1204.

McMahon, T. A. (1975a). Using body size to understand the structural design of animals: quadrupedal locomotion. *J. Appl. Physiol.* **39**, 619–627.

McMahon, T. A. (1975b). Allometry and biomechanics: limb bones in adult ungulates. *Am. Nat.* **109**, 547–563.

McMahon, T. A., Valiant, G. and Frederick, E. C. (1987). Groucho running. *J. Appl. Physiol.* **62**, 2326–2337.

Merkens, H. W., Schamhardt, H. C., Hartman, W. and Kersjes, A. W. (1985). Ground reaction force patterns of Dutch Warmblood horses at normal walk. *Equine Vet. J.* **18**, 207–214.

Moisio, K. C., Sumner, D. R., Shott, S. and Hurwitz, D. E. (2003). Normalization of joint moments during gait: a comparison of two techniques. *J. Biomech.* **36**, 599–603.

Nesbitt, S. J. (2011). The early evolution of archosaurs: relationships and the origin of major clades. *Bull. Am. Museum Nat. Hist.* **352**, 1–292.

Nyakatura, J. A., Andrada, E., Curth, S. and Fischer, M. S. (2014). Bridging "Romer's gap": limb mechanics of an extant belly-dragging lizard inform debate on tetrapod locomotion during the Early Carboniferous. *Evol. Biol.* **41**, 175–190.

Nyakatura, J. A., Melo, K., Horvat, T., Karakasiliotis, K., Allen, V. R., Andikfar, A., Andrada, E., Arnold, P., Lauströer, J., Hutchinson, J. R., et al. (2019). Reverse-engineering the locomotion of a stem amniote. *Nature* **565**, 351–355.

Parrish, J. M. (1986). Locomotor adaptations in the hindlimb and pelvis of the Thecodontia. *Hunteria* **1**, 1–35.

Parrish, J. M. (1987). The origin of crocodilian locomotion. *Paleobiology* **13**, 396–414.

Patel, B. A., Horner, A. M., Thompson, N. E., Barrett, L. and Henzi, S. P. (2013). Ontogenetic scaling of fore- and hind limb posture in wild Chacma baboons (*Papio hamadryas ursinus*). *PLoS ONE* **8**, e71020.

Peters, S. E. (1983). Postnatal development of gait behaviour and functional allometry in the domestic cat (*Felis catus*). *J. Zool.* **199**, 461–486.

Polk, J. D. (2002). Adaptive and phylogenetic influences on musculoskeletal design in cercopithecine primates. *J. Exp. Biol.* **205**, 3399–3412.

Pollock, C. M. and Shadwick, R. E. (1994). Allometry of muscle, tendon, and elastic energy storage capacity in mammals. *Am. J. Physiol.* **266**, R1022-1031.

R Core Team (2020). R: A Language and Environment for Statistical Computing. https://www.r-project.org/

Reilly, S. M. and Blob, R. W. (2003). Motor control of locomotor hindlimb posture in the American alligator (*Alligator mississippiensis*). *J. Exp. Biol.* **206**, 4327–4340.

Reilly, S. M. and Elias, J. A. (1998). Locomotion in *Alligator mississippiensis*: kinematic effects of speed and posture and their relevance to the sprawling-to-erect paradigm. *J. Exp. Biol.* **201**, 2559–2574.

Reilly, S. M., Willey, J. S., Biknevicius, A. R. and Blob, R. W. (2005). Hindlimb function in the alligator: integrating movements, motor patterns, ground reaction forces and bone strain of terrestrial locomotion. *J. Exp. Biol.* **208**, 993–1009.

Reilly, S. M., McElroy, E. J. and Biknevicius, A. R. (2007). Posture, gait and the ecological relevance of locomotor costs and energy-saving mechanisms in tetrapods. *Zoology* **110**, 271–289.

Ren, L., Miller, C. E., Lair, R. and Hutchinson, J. R. (2010). Integration of biomechanical compliance, leverage, and power in elephant limbs. *Proc. Natl. Acad. Sci. U. S. A.* **107**, 7078–7082.

Schmitt, D. (1999). Compliant walking in primates. *J. Zool.* **248**, 149–160.

Schmitt, D. and Hanna, J. B. (2004). Substrate alters forelimb to hindlimb peak force ratios in primates. *J. Hum. Evol.* **46**, 237–252.

Self Davies, Z. T., Spence, A. J. and Wilson, A. M. (2019). Ground reaction forces of overground galloping in ridden Thoroughbred racehorses. *J. Exp. Biol.* **222**, 204107.

Shine, C. L., Penberthy, S., Robbins, C. T., Nelson, O. L. and McGowan, C. P. (2015). Grizzly bear (*Ursus arctos horribilis*) locomotion: gaits and ground reaction forces. *J. Exp. Biol.* **218**, 3102–3109.

Singh, L. A. K. and Bustard, H. R. (1976). Locomotory behaviour during basking and spoor formation in the gharial (*Gavialis gangeticus*). *Br. J. Herpetol.* **5**, 673–676.

Sullivan, C. S. (2007). Function and evolution of the hind limb in Triassic archosaurian reptiles. Ph.D. dissertation, Harvard University, Cambridge. 267 pp.

Turnquist, J. E. and Wells, J. P. (1994). Ontogeny of locomotion in rhesus macaques (*Macaca mulatta*): I. Early postnatal ontogeny of the musculoskeletal system. *J. Hum. Evol.* **26**, 487–499.

Vilensky, J. A. and Gankiewicz, E. (1989). Early development of locomotor behavior in vervet monkeys. *Am. J. Primatol.* **17**, 11–25.

Willey, J. S., Biknevicius, A. R., Reilly, S. M. and Earls, K. D. (2004). The tale of the tail: limb function and locomotor mechanics in *Alligator mississippiensis*. *J. Exp. Biol.* **207**, 553–563.

Wiseman, A. L. A., Bishop, P. J., Demuth, O. E., Cuff, A. R., Michel, K. B. and Hutchinson, J. R. (2021). Musculoskeletal modelling of the Nile crocodile (*Crocodylus niloticus*) hindlimb: effects of limb posture on leverage during terrestrial locomotion. *J. Anat.* **239**, 424–444.

Young, J. W. (2009). Ontogeny of joint mechanics in squirrel monkeys (*Saimiri boliviensis*): Functional implications for mammalian limb growth and locomotor development. *J. Exp. Biol.* **212**, 1576–1591.

Young, J. W. (2012). Ontogeny of limb force distribution in squirrel monkeys (*Saimiri boliviensis*): insights into the mechanical bases of primate hind limb dominance. *J. Hum. Evol.* **62**, 473–485.

Young, J. W. and Shapiro, L. J. (2018). Developments in development: what have we learned from primate locomotor ontogeny? *Am. J. Phys. Anthropol.* **165**, 37–71.

Zeininger, A., Shapiro, L. J. and Raichlen, D. A. (2017). Ontogenetic changes in limb postures and their impact on effective limb length in baboons (*Papio cynocephalus*). *Am. J. Phys. Anthropol.* **163**, 231–241.

Zumwalt, A. C., Hamrick, M. and Schmitt, D. (2006). Force plate for measuring the ground reaction forces in small animal locomotion. *J. Biomech.* **39**, 2877–2881.

Figures

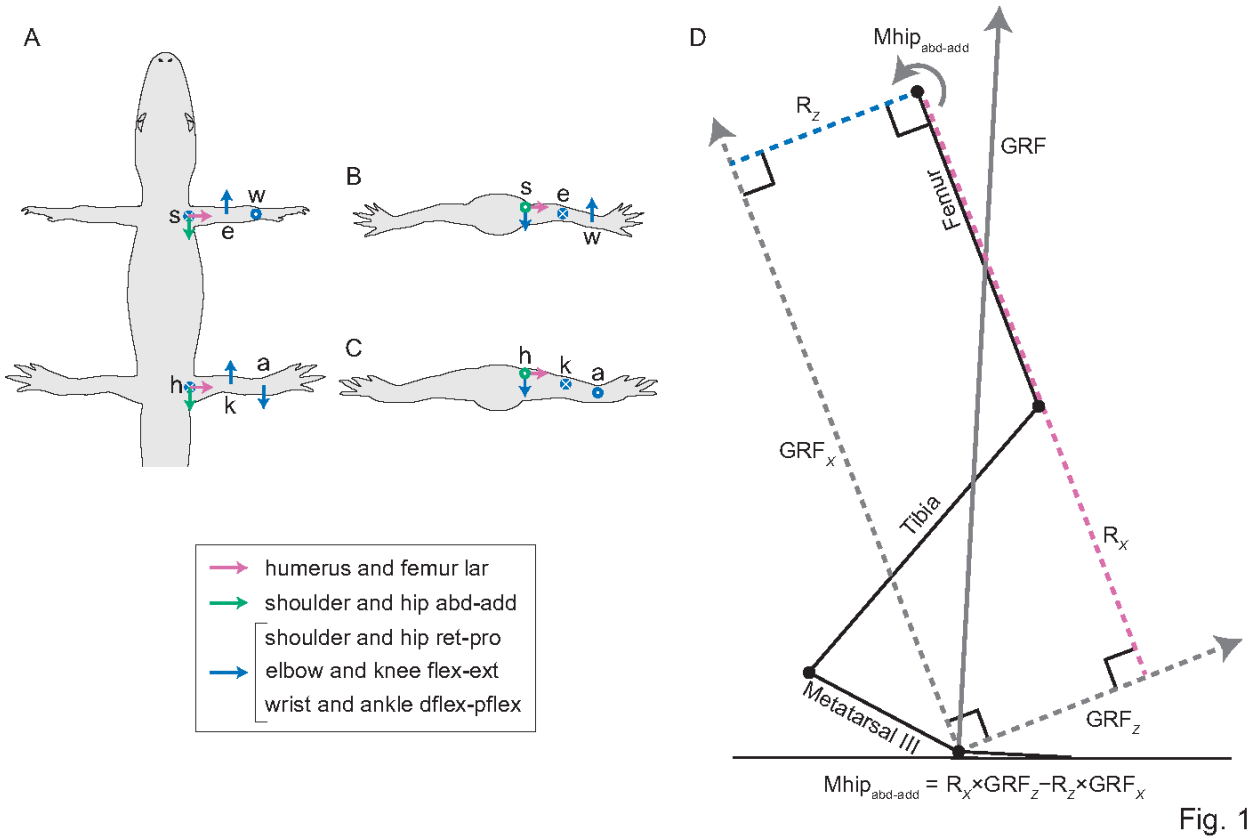

Fig. 1

Fig. 1. The reference pose and joint coordinate systems for fore- and hindlimbs and an example of the joint moment calculation. (A) dorsal view of the body, and (B and C) posterior views of fore- and hindlimbs, respectively. *x*- (pink), *y*- (green), and *z*- (blue) rotational axes represent long axis rotation, abduction-adduction, and retraction-protraction (for shoulder and hip) or flexion-extension (for distal joints), respectively. Right-hand rule convention (counterclockwise positive and clockwise negative rotation as viewed from the arrow head) was used. The circled dot and circled × indicate the arrow head and the opposite end, respectively. (D) calculation of the hip abduction-adduction moment ($Mhip_{abd\text{-}add}$). The

ground reaction force (GRF) was resolved into two components parallel to the long axis of the femur (GRF_x) and the hip retraction-protraction axis (GRF_z). Given that the moment arms of GRF_x and GRF_z about the rotational axis are R_z and R_x, respectively, $Mhip_{abd\text{-}add}$ was calculated as $R_x \times GRF_z - R_z \times GRF_x$. Joint abbreviations: a, ankle; e, elbow; h, hip; k, knee; s, shoulder; w, wrist. Limb movement abbreviations: abd, abduction; add, adduction; dflex, dorsiflexion; ext, extension; flex, flexion; lar, long axis rotation; pflex, plantarflexion; pro, protraction; ret, retraction.

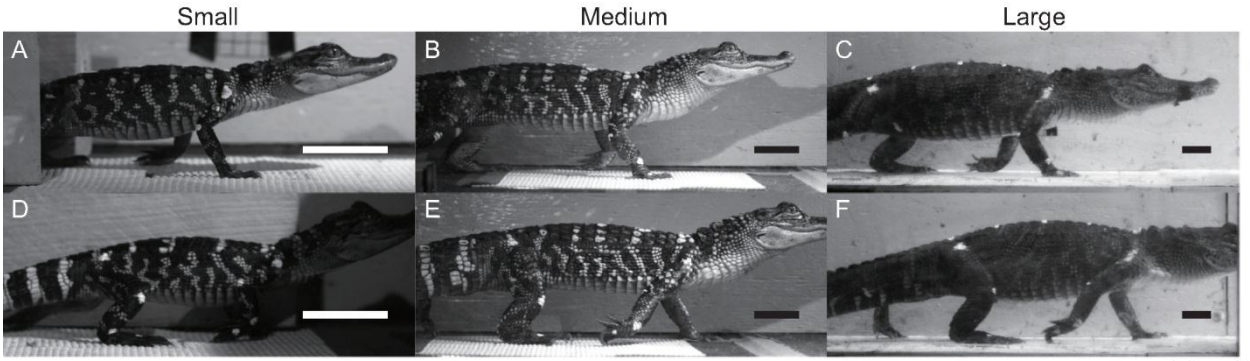

Fig. 2

Fig. 2. Comparisons of mid-stance limb posture among three size classes of American alligators. Forelimb posture (A–C, from left to right), and hindlimb posture (D–F, from left to right) for small, medium, and large alligators. Scale bars are 5 cm.

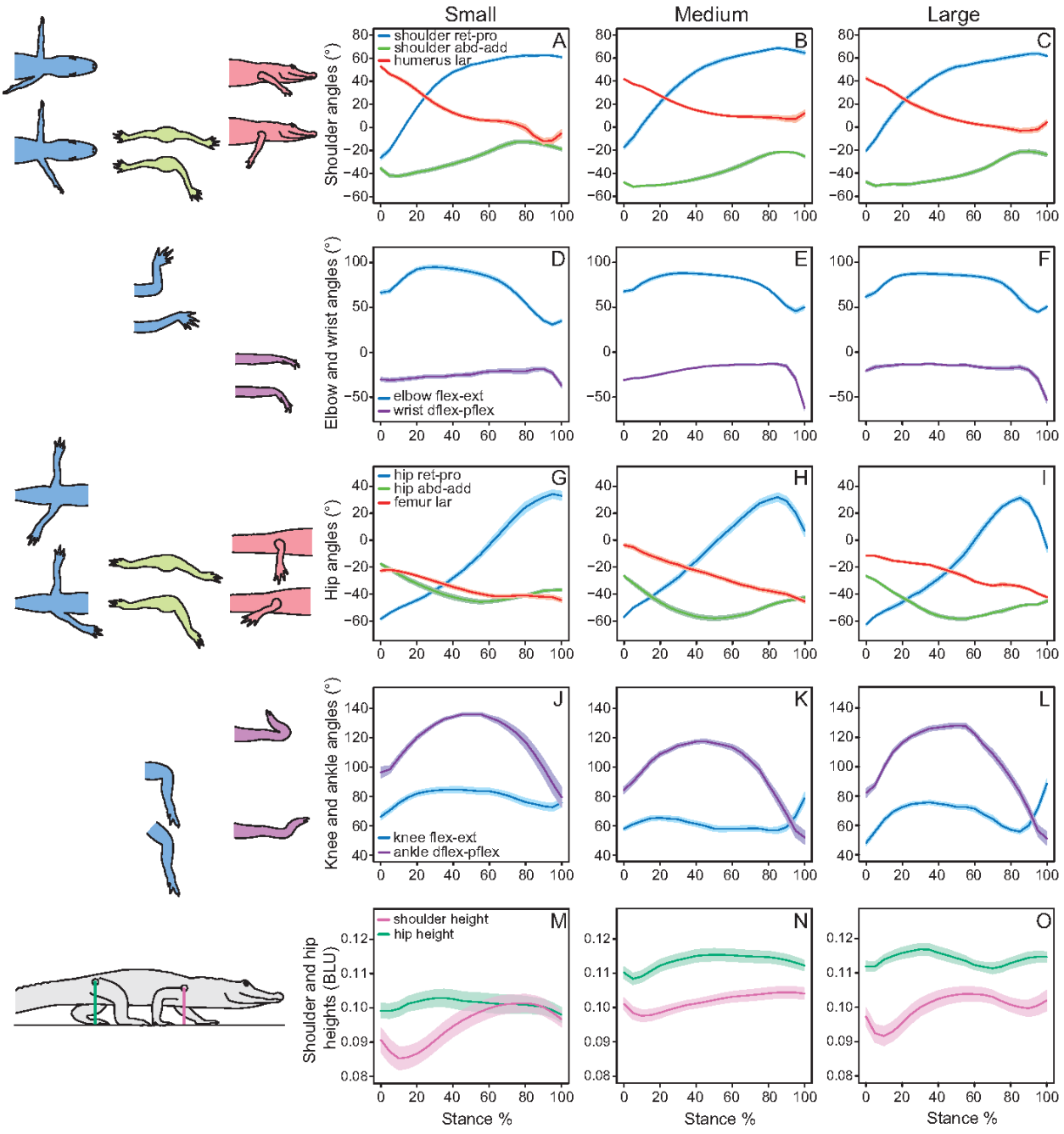

Fig. 3

Fig. 3. Fore- and hindlimb angles and shoulder and hip heights throughout stance in three size classes of American alligators. (A–C) shoulder angles, (D–F) elbow and wrist angles, (G–I) hip angles, (J–L) knee and ankle angles, and (M–O) shoulder and hip heights in body

length unit (BLU). Lines and shaded areas represent mean traces and their standard errors, respectively. Note that humerus and femur long axis rotation is affected by elbow and knee abduction-adduction that was not accounted for, and flexion-extension axes of the elbow, wrist, knee, and ankle change with respect to osteologically defined joint axes during stance. Limb movement abbreviations: abd, abduction; add, adduction; dflex, dorsiflexion; ext, extension; flex, flexion; lar, long axis rotation; pflex, plantarflexion; pro, protraction; ret, retraction. Lines and shaded areas represent mean traces and their standard errors, respectively. See text for sample sizes for each size class.

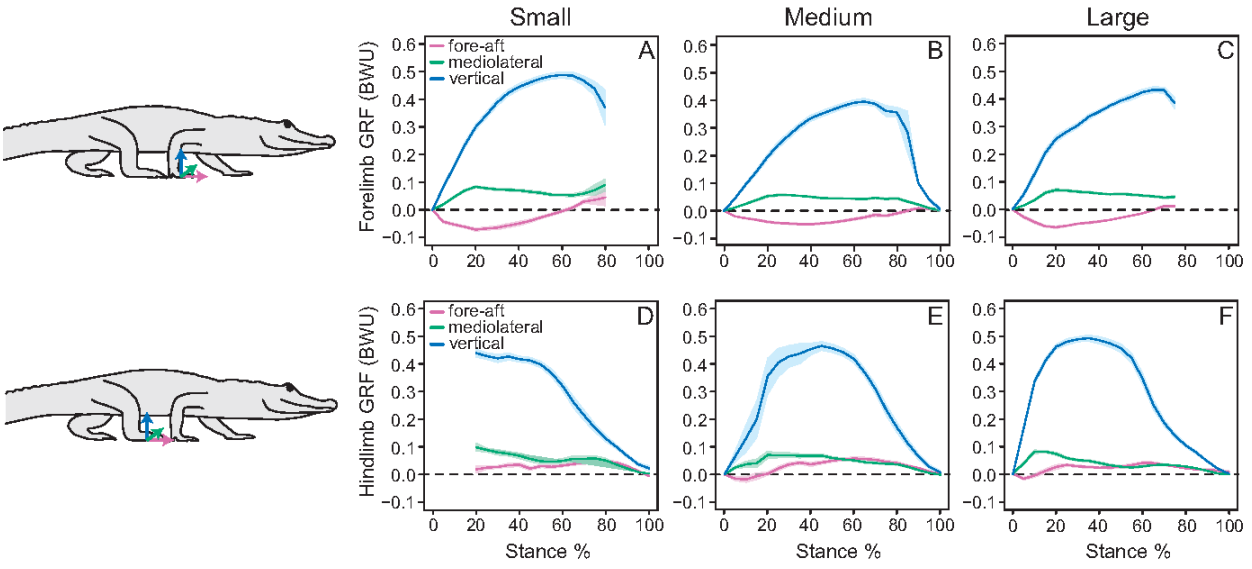

Fig. 4. Fore- and hindlimb forces throughout stance in three size classes of American alligators. (A–C) Forelimb GRF, and (D–F) hindlimb GRF in body weight units (BWU). Lines and shaded areas represent mean traces and their standard errors, respectively. See text for sample sizes for each size class.

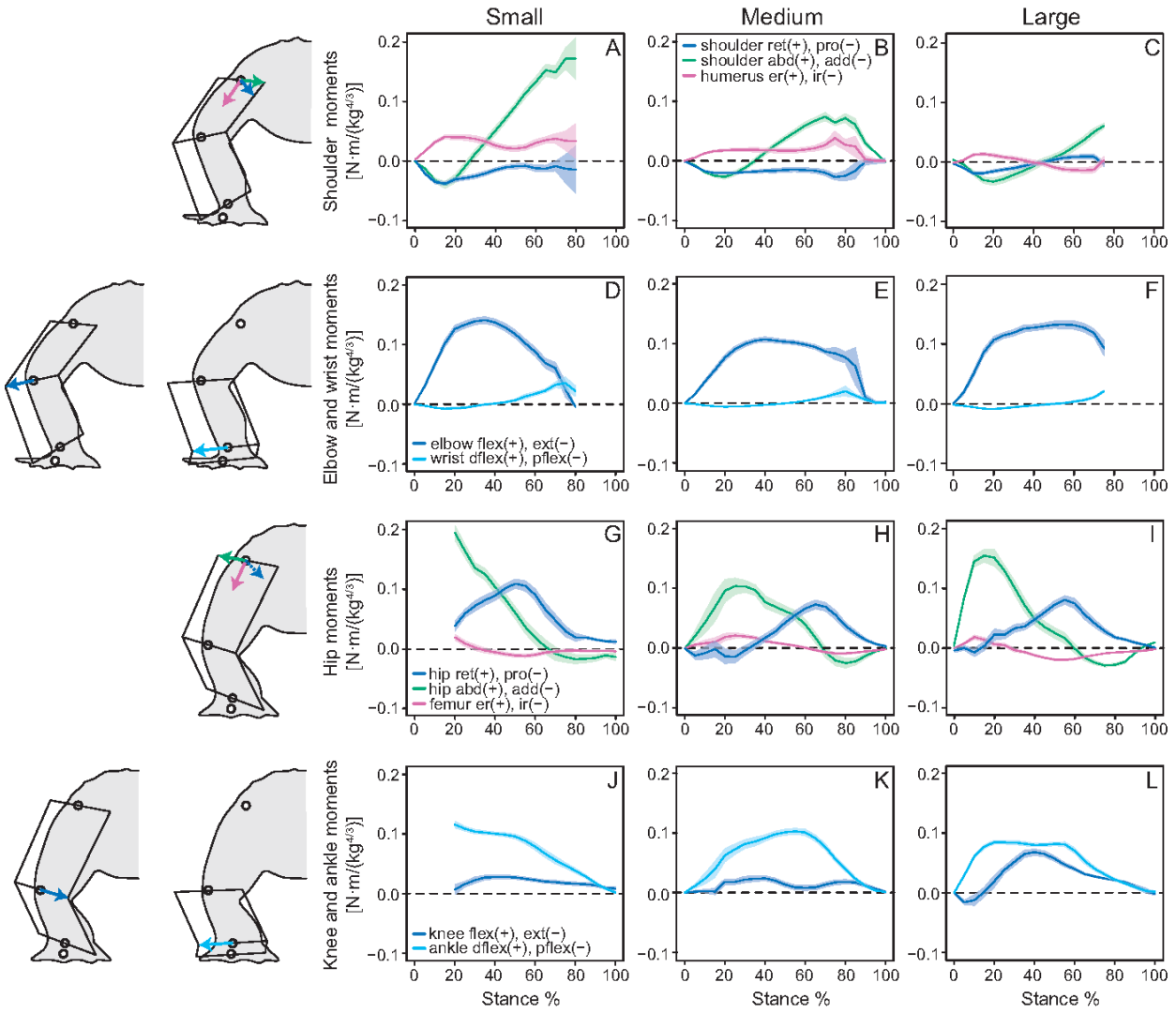

Fig. 5. Fore- and hindlimb joint moments exerted by the GRF throughout stance in three size classes of American alligators. (A–C) Shoulder moments, (D–F) elbow and wrist moments, (G–I) hip moments, and (J–L) knee and ankle moments. Moments are in normalized units [$N{\cdot}m/(kg^{4/3})$]. Lines and shaded areas represent mean traces and their standard errors, respectively. Joint moment abbreviations: abd, abduction; add, adduction; dflex, dorsiflexion; er, external rotation; ext, extension; flex, flexion; ir, internal rotation; pflex, plantarflexion; pro, protraction; ret, retraction. See text for sample sizes for each size class.

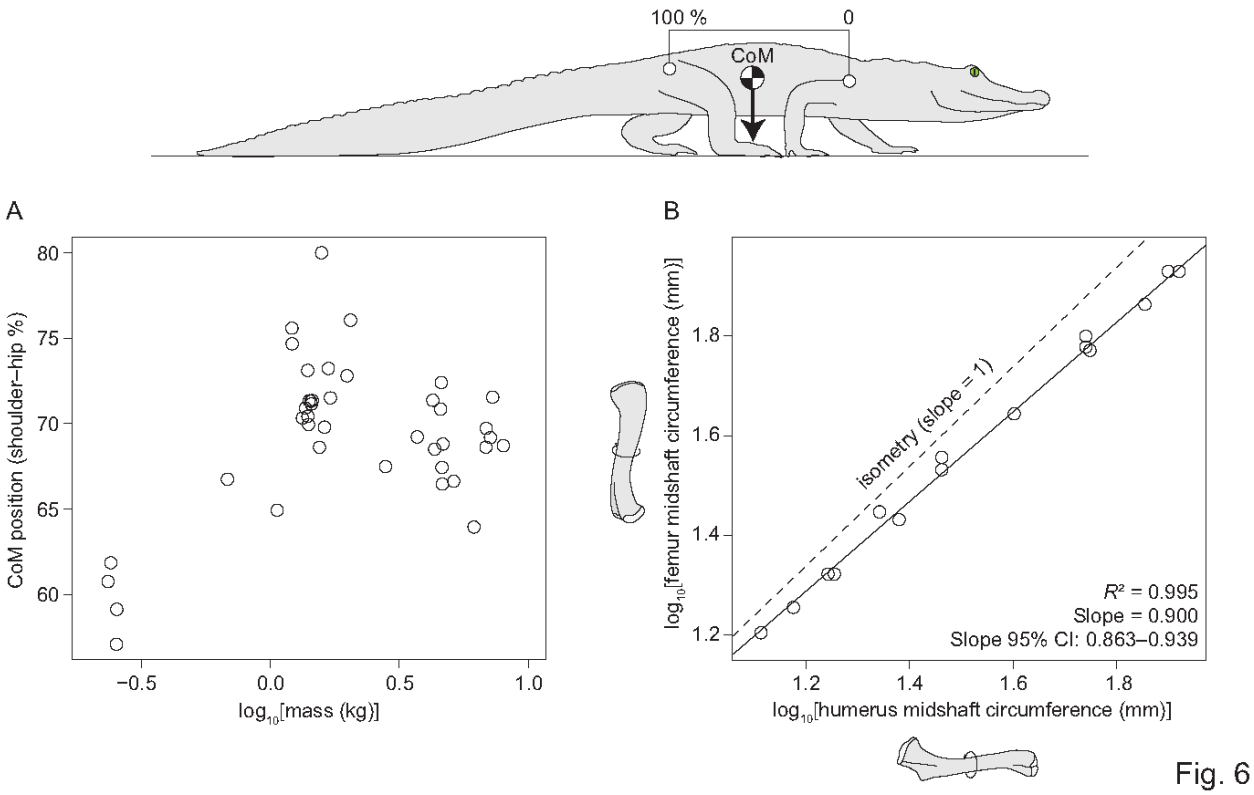

Fig. 6. Ontogenetic changes in the CoM and limb morphology in American alligators. (A) CoM position (shoulder–hip %) vs. body mass, and (B) femur vs. humerus midshaft circumferences. Each data point in (A) represents a single individual (n = 12). Data depicted in (B) from Iijima and Kubo (2019).

Table 1. Comparisons of speed and stride parameters among three size classes

	Dimensionless speed $[u(g \cdot h)^{-0.5}]$	Stride duration (s)	Duty factor	Stride length (BLU)
Forelimb				
Small class mean±s.e.m.	0.194±0.008	1.226±0.041	0.718±0.012	0.347±0.011
Medium class mean±s.e.m.	0.138±0.012	1.943±0.117	0.722±0.010	0.246±0.006
Large class mean±s.e.m.	0.128±0.010	2.573±0.155	0.734±0.013	0.291±0.006
LME model Ω^2	0.277	0.872	0.022	0.591
ANOVA *p*	0.001	0.004	0.817	0.002
Small vs. medium z	4.239	-1.479	0.164	4.249
Small vs. large z	4.363	-4.013	-0.406	1.709
Medium vs. large z	0.639	-2.988	-0.615	-1.512
Small vs. medium *p*	0.000	0.298	0.985	<0.001
Small vs. large *p*	0.000	<0.001	0.913	0.199
Medium vs. large *p*	0.798	0.008	0.811	0.282
Hindlimb				
Small class mean±s.e.m.	0.176±0.009	1.416±0.063	0.740±0.012	0.373±0.014
Medium class mean±s.e.m.	0.144±0.010	1.873±0.116	0.788±0.008	0.262±0.005
Large class mean±s.e.m.	0.104±0.009	3.146±0.226	0.834±0.009	0.285±0.004
LME model Ω^2	0.347	0.835	0.560	0.679
ANOVA *p*	0.001	0.001	0.015	0.005
Small vs. medium z	2.541	0.054	-2.030	3.704
Small vs. large z	5.641	-4.559	-3.099	1.971
Medium vs. large z	3.096	-5.376	-1.638	-0.786
Small vs. medium *p*	0.030	0.998	0.104	0.001
Small vs. large *p*	<0.001	0.000	0.005	0.117
Medium vs. large *p*	0.005	<0.001	0.228	0.709

Linear mixed effects (LME) models were used with size class and dimensionless speed as fixed effects and individual as a random effect. For the comparison of dimensionless speed, only size class was used as a fixed effect. The effect of size class was tested by ANOVA comparing the models with and without size class as a fixed effect. BLU, body length unit. See text for sample sizes in each size class.

Table 2. Comparisons of fore- and hindlimb joint angles among three size classes

Forelimb	Humerus retraction-protraction angle (max–min °)	Humerus adduction angle (mean °)	Humerus long axis rotation (max–min °)	Elbow flexion angle (mean °)	Wrist plantarflexion angle (mean °)
Small class mean±s.e.m.	92.0±2.0	-25.9±1.7	68.2±2.6	86.3±2.5	-24.0±2.0
Medium class mean±s.e.m.	87.4±1.8	-39.3±1.4	39.6±2.3	84.8±1.5	-16.3±0.7
Large class mean±s.e.m.	85.6±2.2	-40.9±1.2	47.5±2.7	84.7±2.0	-15.4±1.1
LME model Ω^2	0.200	0.702	0.545	0.288	0.399
ANOVA *p*	0.241	0.011	0.000	0.753	0.068
Small vs. medium z	-1.089	-2.771	-8.406	-0.603	1.967
Small vs. large z	-1.268	-2.212	-5.591	-0.507	1.663
Medium vs. large z	0.444	0.273	-1.864	0.076	-0.212
Small vs. medium *p*	0.518	0.015	<0.001	0.816	0.118
Small vs. large *p*	0.410	0.067	<0.001	0.866	0.216
Medium vs. large *p*	0.896	0.959	0.148	0.997	0.975
Hindlimb	Femur retraction-protraction angle (max–min °)	Femur adduction angle (mean °)	Femur long axis rotation (max–min °)	Knee flexion angle (mean °)	Ankle dorsiflexion angle (mean °)
Small class mean±s.e.m.	95.9±3.3	-42.5±1.5	26.1±1.3	83.0±2.2	131.3±1.4
Medium class mean±s.e.m.	87.3±3.1	-55.0±1.6	42.7±1.6	60.1±1.9	112.2±1.6
Large class mean±s.e.m.	95.7±2.0	-54.8±0.8	33.2±1.2	71.2±1.5	120.7±1.5
LME model Ω^2	0.556	0.659	0.612	0.624	0.617
ANOVA *p*	0.651	0.008	0.000	0.000	0.000
Small vs. medium z	-0.428	-3.157	7.852	-6.541	-7.038
Small vs. large z	0.367	-2.359	1.477	-3.143	-3.537
Medium vs. large z	-0.679	0.059	5.815	-1.998	-2.119
Small vs. medium *p*	0.903	0.005	<0.001	<0.001	<0.001
Small vs. large *p*	0.927	0.047	0.300	0.005	0.001
Medium vs. large *p*	0.773	0.998	<0.001	0.111	0.085

Larger absolute values indicate larger angles of interest. Mean angles were taken from 25–75 % of stance. Linear mixed effects (LME) models were used with size class and dimensionless speed as fixed effects and individual as a random effect. The effect of size class was tested by ANOVA comparing the models with and without size class as a fixed effect. See text for sample sizes in each size class.

Table 3. Comparisons of peak fore- and hindlimb forces and GRF medial inclination angles among three size classes

	Peak vertical force (BWU)	Peak propulsive force (BWU)	Peak braking force (BWU)	Peak medial force (BWU)	GRF medial inclination angle (°)
Forelimb					
Small class mean±s.e.m.	0.510±0.011	0.040±0.005	-0.098±0.007	0.114±0.005	8.1±0.5
Medium class mean±s.e.m.	0.413±0.010	0.007±0.002	-0.059±0.004	0.071±0.004	8.5±0.4
Large class mean±s.e.m.	0.441±0.011	0.025±0.003	-0.075±0.003	0.080±0.005	8.7±0.6
LME model Ω^2	0.385	0.315	0.297	0.523	0.108
ANOVA *p*	0.000	0.002	0.002	0.006	0.397
Small vs. medium z	5.560	4.999	-3.882	3.326	-0.796
Small vs. large z	3.370	2.004	-1.693	1.797	-0.958
Medium vs. large z	-1.503	-2.484	1.688	-0.797	-0.339
Small vs. medium *p*	<0.001	<0.001	0.000	0.003	0.704
Small vs. large *p*	0.002	0.111	0.207	0.169	0.601
Medium vs. large *p*	0.289	0.035	0.209	0.703	0.938
Hindlimb					
Small class mean±s.e.m.	0.461±0.012	0.072±0.006	-0.016±0.003	0.116±0.012	11.0±1.2
Medium class mean±s.e.m.	0.507±0.015	0.074±0.006	-0.011±0.003	0.094±0.005	9.0±1.0
Large class mean±s.e.m.	0.517±0.009	0.068±0.008	-0.011±0.003	0.070±0.005	6.8±0.6
LME model Ω^2	0.174	0.094	0.051	0.259	0.144
ANOVA *p*	0.019	0.619	0.521	0.090	0.033
Small vs. medium z	-2.778	-0.647	-0.996	1.163	1.596
Small vs. large z	-3.069	-0.639	-0.745	1.850	2.829
Medium vs. large z	-0.835	-0.126	0.079	0.995	1.691
Small vs. medium *p*	0.015	0.793	0.577	0.473	0.246
Small vs. large *p*	0.006	0.797	0.735	0.152	0.013
Medium vs. large *p*	0.680	0.991	0.997	0.578	0.207

GRF medial inclination angles were taken from 25–75 % of stance. Linear mixed effects models (LME) were used with size class and dimensionless speed as fixed effects and individual as a random effect. The effect of size class was tested by ANOVA comparing the models with and without size class as a fixed effect. BWU, body weight unit. See text for sample sizes in each size class.

Table 4. Comparisons of peak fore- and hindlimb joint moments among three size classes

Forelimb	Shoulder protraction moment	Shoulder abduction moment	Humerus external rotation moment	Humerus internal rotation moment	Elbow flexion moment	Wrist dorsiflexion moment
Small class mean±s.e.m.	-0.050±0.004	0.169±0.009	0.055±0.005	-0.009±0.003	0.154±0.006	0.030±0.004
Medium class mean±s.e.m.	-0.029±0.002	0.086±0.005	0.032±0.004	-0.003±0.002	0.117±0.004	0.012±0.002
Large class mean±s.e.m.	-0.020±0.002	0.051±0.006	0.019±0.003	-0.018±0.004	0.139±0.007	0.015±0.003
LME model Ω^2	0.507	0.756	0.462	0.148	0.259	0.259
ANOVA *p*	0.016	0.004	0.032	0.016	0.001	0.047
Small vs. medium z	2.229	3.088	-1.709	1.653	-4.228	-2.272
Small vs. large z	2.603	3.127	-2.239	-1.688	-1.395	-1.369
Medium vs. large z	-0.911	-0.903	0.952	3.356	-2.440	-0.426
Small vs. medium *p*	0.065	0.006	0.199	0.223	<0.001	0.059
Small vs. large *p*	0.025	0.005	0.064	0.209	0.342	0.355
Medium vs. large *p*	0.631	0.635	0.604	0.002	0.039	0.904
Hindlimb	Hip retraction moment	Hip abduction moment	Femur external rotation moment	Femur internal rotation moment	Knee flexion moment	Ankle dorsiflexion moment
Small class mean±s.e.m.	0.119±0.006	0.175±0.009	0.015±0.003	-0.021±0.003	0.040±0.002	0.112±0.003
Medium class mean±s.e.m.	0.083±0.007	0.117±0.008	0.024±0.003	-0.011±0.002	0.039±0.004	0.109±0.004
Large class mean±s.e.m.	0.090±0.007	0.152±0.008	0.014±0.002	-0.022±0.002	0.075±0.005	0.094±0.003
LME model Ω^2	0.301	0.311	0.192	0.333	0.498	0.425
ANOVA *p*	0.030	0.001	0.086	0.005	0.001	0.547
Small vs. medium z	-2.402	4.683	1.560	3.259	-0.361	-0.096
Small vs. large z	-1.146	2.012	-0.084	0.469	4.114	-0.801
Medium vs. large z	-0.747	2.045	1.361	2.249	-4.819	0.744
Small vs. medium *p*	0.043	<0.001	0.260	0.003	0.930	0.995
Small vs. large *p*	0.483	0.108	0.996	0.885	0.000	0.699
Medium vs. large *p*	0.733	0.101	0.359	0.062	<0.001	0.735

Normalized joint moments [$N{\cdot}m/(kg^{4/3})$] were compared. Larger absolute values indicate larger moments of interest. Linear mixed effects (LME) models were used with size class and dimensionless speed as fixed effects and individual as a random effect. The effect of size class was tested by ANOVA comparing the models with and without size class as a fixed effect. See text for sample sizes in each size class.

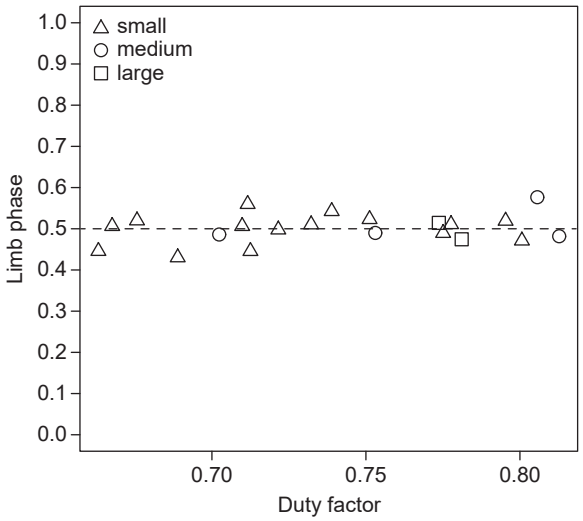

Fig. S1. **Relationship between limb phase (Hildeb-rand, 1976) and duty factor in three size classes of American alligators.** Comparisons include trials in which steady-speed fore- and hindlimb steps were filmed in a single video.

Table S1. Sensitivity analysis of peak fore- and hindlimb joint moments in al09f21 (2.06 kg body mass) using either the dorsal, ventral, anterior, and posterior edge of each fore- and hindlimb joint landmark.

Forelimb	Shoulder protraction moment	Shoulder abduction moment	Humerus external rotation moment	Humerus internal rotation moment	Elbow flexion moment	Wrist dorsiflexion moment
al09f21	-0.044	0.080	0.035	0.000	0.124	0.007
al09f21_dorsal	-0.046	0.094	0.039	0.000	0.126	0.003
al09f21_ventral	-0.052	0.078	0.046	0.000	0.122	0.011
al09f21_anterior	-0.038	0.092	0.037	0.000	0.125	0.008
al09f21_posterior	-0.043	0.077	0.041	0.000	0.123	0.010
% difference from al09f21						
al09f21_dorsal	4.0	18.3	10.1	0.0	1.9	53.4
al09f21_ventral	17.9	2.3	28.8	0.0	1.1	41.9
al09f21_anterior	14.7	15.7	3.6	0.0	0.7	11.0
al09f21_posterior	2.9	3.6	16.6	0.0	0.4	32.8
Average % difference	9.9	10.0	14.8	0.0	1.0	34.8
Hindlimb	Hip retraction moment	Hip abduction moment	Femur external rotation moment	Femur internal rotation moment	Knee flexion moment	Ankle dorsiflexion moment
al09f21	0.114	0.127	0.021	-0.003	0.033	0.100
al09f21_dorsal	0.115	0.129	0.025	-0.004	0.047	0.096
al09f21_ventral	0.107	0.126	0.018	-0.002	0.020	0.103
al09f21_anterior	0.118	0.127	0.018	-0.002	0.023	0.101
al09f21_posterior	0.111	0.137	0.025	-0.003	0.036	0.104
% difference from al09f21						
al09f21_dorsal	0.9	1.5	16.5	42.4	42.7	3.9
al09f21_ventral	5.8	0.9	18.2	37.7	38.9	2.6
al09f21_anterior	3.6	0.0	16.7	40.9	30.3	1.3
al09f21_posterior	2.3	8.4	17.7	2.1	10.2	3.6
Average % difference	3.1	2.7	17.3	30.8	30.6	2.8

Normalized joint moments [$N \cdot m/(kg^{4/3})$] were compared. Larger absolute values indicate larger moments of interest.

Table S2. Ordinary least squares regressions of the ankle dorsiflexion moment on the femur adduction angle in each individual

Size class	Individual	*n*	R^2	Elevation	Slope	*P* value
Small	al10	9	0.314	0.027	-0.001	0.117
	al11	9	0.438	0.028	-0.002	0.052
	al12	4	0.144	0.092	-0.001	0.621
Medium	al07	8	0.519	-0.044	-0.003	0.044
	al08	4	0.474	-0.026	-0.002	0.311
	al09	9	0.074	0.030	-0.001	0.480
Large	al05	20	0.108	0.039	-0.001	0.157

Normalized moments [$N \cdot m / (kg^{4/3})$] and angles were taken from mid-stance. Negative slopes indicate that more adducted (upright) postures have larger dorsiflexion moments at the ankle.

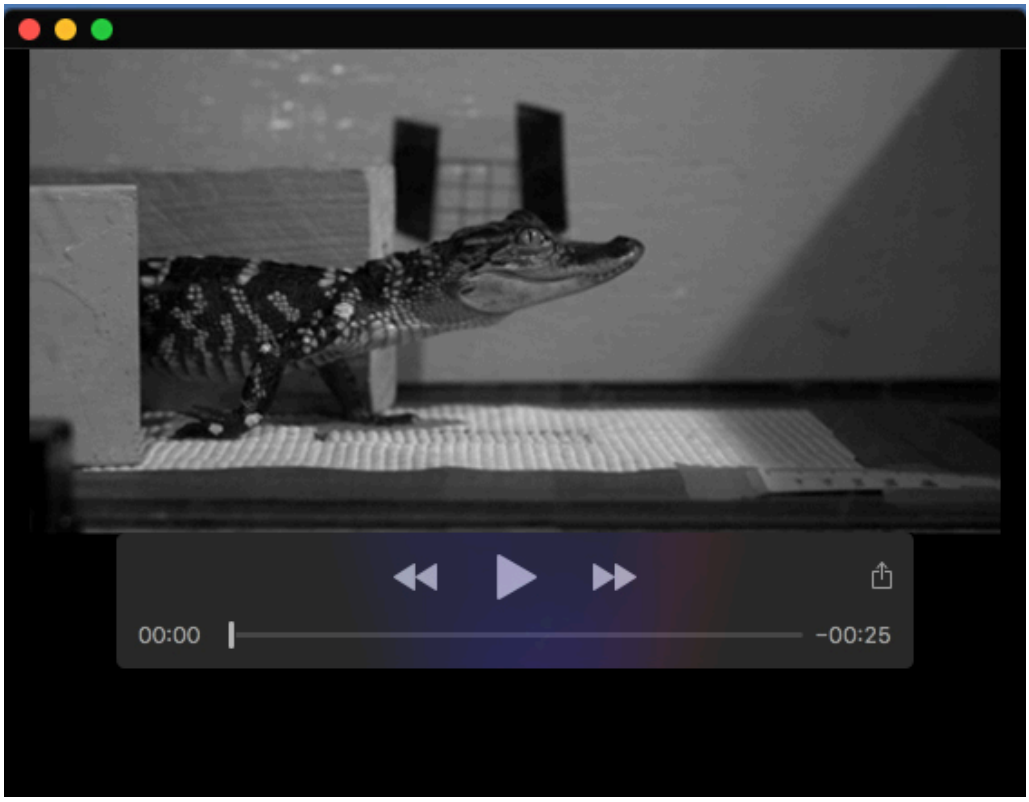

Movie 1. Representative walk (al10f18) of a small size alligator (0.1× speed).

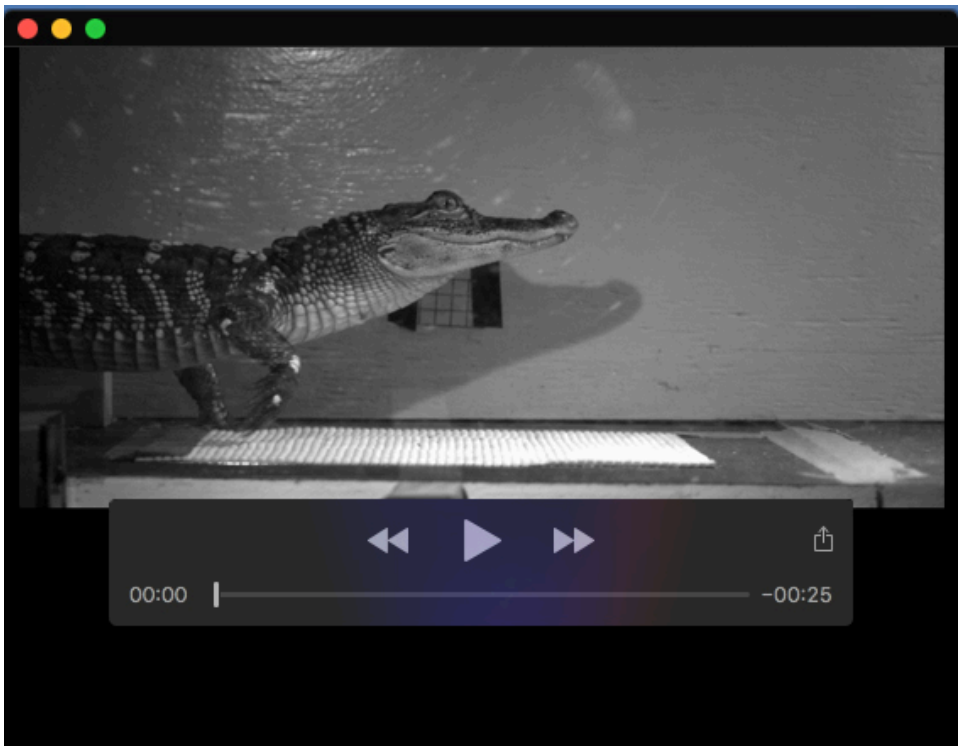

Movie 2. Representative walk (al09f21) of a medium size alligator (0.1× speed).

Movie 3. Representative walk (al05f77) of a large size alligator (0.1× speed).